Title
Kinematics and thermodynamics of a growing rim of high-pressure phase

Author
Morris, SJS

Publication Date
2014-03-01

DOI
10.1016/j.pepi.2014.01.003

Peer reviewed

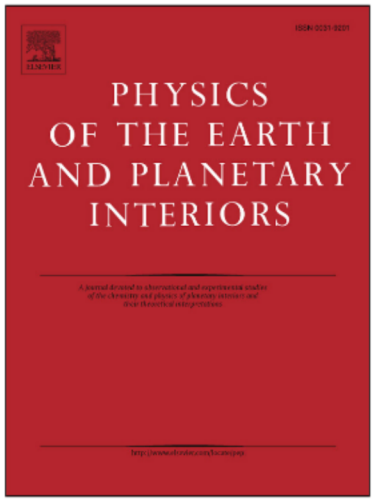

Kinematics and thermodynamics of a growing rim of high–pressure phase

S.J.S. Morris

PII: S0031-9201(14)00004-1
DOI: http://dx.doi.org/10.1016/j.pepi.2014.01.003
Reference: PEPI 5702

To appear in: *Physics of the Earth and Planetary Interiors*

Received Date: 25 February 2013
Revised Date: 4 January 2014
Accepted Date: 7 January 2014

Please cite this article as: Morris, S.J.S., Kinematics and thermodynamics of a growing rim of high–pressure phase, *Physics of the Earth and Planetary Interiors* (2014), doi: http://dx.doi.org/10.1016/j.pepi.2014.01.003

Kinematics and thermodynamics of a growing rim of high–pressure phase

S. J. S. Morris[a]

[a] *Department of Mechanical Engineering, University of California Berkeley, CA 94720, USA*

Abstract

We have reanalysed the problem of growth of a dense product rim on a sphere of parent phase. To decouple the problem of calculating deformation from rheology, we assume spherical symmetry, and incompressible phases. Within the product, the radial deviatoric strain and its time–derivative prove to be of opposite sign: strain is compressive, but the strain rate is tensile. Further, the radial deviatoric strain in the new product adjacent to the interface is invariant in time. Propagation of the phase interface is determined by a competition between two mechanisms: as an element of material is transformed, its shear strain energy is increased; and the core pressure performs work compressing it. For elastic phases, this competition results in metastability. Within a certain pressure range, either phase can occur alone, but the two phases can not coexist. Because this result is inconsistent with experiments by Kubo et al. (1998a) in which a rim of high–pressure phase (wadsleyite) coexists with a central core of low–pressure phase (olivine), we then incorporate plastic flow. Assuming perfect plasticity, we show that for a given applied pressure exceeding the coexistence pressure, a rim of product can now nucleate if the excess pressure Δp exceeds a critical value depending on yield stress. Increasing Δp above this value allows product to grow into the parent phase. There are now two possibilities, depending on the value of Δp. Growth may eventually cease to produce a state in which the product rim is in equilibrium with a parent core; or growth may follow a more complicated path: within a range of excess pressures, the growth rate can decrease strongly from its initial value to produce a quasi–equilibrium state, before increasing again to a rate similar to that at which transformation began. We interpret these results to mean that if Δp is increased slowly in a series of experiments with constant yield stress, the sample passes through a series of equilibria until Δp is large enough for the second type of growth to be possible; transformation is then completed rapidly on the timescale set by interface kinetics. This result may be relevant to the problem of deep earthquakes. Lastly, using existing experiments in which a wadsleyite rim grows on an olivine sphere, we apply the theory to estimate the yield strength of wadsleyite: our estimates are consistent with measurements by independent methods.

1. Introduction

In reviewing the experimental evidence for coupling of transformation stress and interface kinetics during metamorphism, Rubie & Thompson (1985, p.58) suggest that 'a reaction involving volume increase and proceeding at pressures below the equilibrium boundary will be characterized by localized stress development around a growing nucleus. This may result in a localized pressure increase back towards equilibrium. Then ... the growth rate slows. Transformation stress is expected to produce initially elastic and later plastic strain in the reacting system'. This passage is often quoted (e.g. by Morris 2002) or paraphrased; see Rubie & Champness (1987), Kubo et al. (1998), Mosenfelder & Bohlen (1997) and Schmid et al. (2009).

For the olivine–spinel transformation, time–dependent growth rates have been demonstrated by Kubo et al. (1998a). Millimetre cubes of single crystal olivine were subjected to a constant pressure exceeding the coexistence pressure of the olivine and wadsleyite phases. A thin rim of wadsleyite nucleated on the sample surface and grew inwards to consume the parent olivine phase. In their series at 1503 K and 14 GPa, the interface speed decreased by at least a factor of 60 over 600 minutes; and in the series at 1303 K and 13.5 GPa, the rim ceased to grow at a width of about 50 μm. The experiments demonstrate time–dependent growth rates. They do not support the suggestion that strain is 'initially elastic', however.

As discussed by Kubo et al.(1998b, p.86), microstructural evidence suggests that plastic deformation was essential to allowing even the limited rim growth occurring in the series at 13.5 GPa. The rim thickness at 600 minutes increased 4–fold when the water content of the wadsleyite rim was increased from 200 ppmw to 500 ppmw at fixed temperature and pressure. The dislocation structures within the wadsleyite rim also differed. For the run at 200 ppmw, the dislocation density was larger (10^{13} to 10^{14} m^{-2}), and the dislocations were tangled. Kubo et al.(1998a, p.5) interpret this evidence to mean that the rim at first deformed plastically, and that growth ceased when hardening had increased the strength sufficiently. For the run at 500 ppmw, the dislocation density was an order of magnitude less, and subgrain boundaries were observed; the authors interpret these textures to mean that dislocations recovered, permitting more rapid flow. This evidence is consistent with deformation occurring by dislocation creep; that is by dislocation glide in the experiments at 200 ppmw, and by dislocation glide or climb (or a combination thereof) in the experiments at 500 ppmw. In similar experiments at 1373 K and 16 GPa, Mosenfelder et al.(2000, p.67) observed well–defined dislocation cells; they infer that 'deformation occurred by dislocation creep, although it is not clear whether the rate of climb or the rate of glide was rate–controlling'. Both studies conclude that dislocation creep occurred; the only difference is that Mosenfelder et al.(2000) observed dislocation cells. Because neither study saw any evidence that diffusion creep was a significant process, in the rest of this paper, the terms 'creep' and 'dislocation creep' are used interchangeably.

Though microstructural evidence suggests that plastic deformation is essen-

tial to rim growth, current models support the Rubie and Thompson notion that strain is initially elastic. Assuming ideal plasticity, Mosenfelder et al. (2000) analyse rim growth on a sphere. The strain is predicted to be purely elastic at first; plastic strain becomes non–zero only after the rim has reached a certain thickness depending on yield stress. Because that conclusion is not consistent with microstructural evidence, here we reanalyse the problem of rim growth. As in my previous papers on this topic, the motion is assumed to be spherically–symmetric; and the phases are taken to be incompressible: the density of each phase is uniform in space and in time. As noted by Morris (1992), with these assumptions, the deformation is determined kinematically; it is independent of constitutive assumptions. Using this approach, we can discuss carefully the displacements and strain. With the kinematics understood, we then introduce the constitutive assumption and the thermodynamics needed to close the model.

This approach allows us to clarify the two issues involved in the modelling. The first is the correct formulation of the constitutive equation. By this I do not mean a choice between models such viscoelasticity, or ideal plasticity; the issue is rather that of using the correct independent variables to formulate *whatever* model one subsequently chooses. In the appendix, we use examples from the literature to show that making an incorrect choice at this point can result in a model that violates causality. The second issue is the correct formulation of the kinetic relation; if this is not done correctly, the second law of thermodynamics is violated at the phase interface. As given by Vaughan et al.(1984), the correct formulation is local in the sense that it depends only on conditions evaluated within each phase at the phase interface. The Vaughan et al. formulation imposes the laws of thermodynamics at the phase interface. By contrast, Liu et al.(1998) use, without proof or citing a derivation, a different kinetic equation. There is no reason to believe that their kinetic equation is consistent with the laws of thermodynamics.

The logic of this paper is as follows. In §2, we analyse the kinematics of spherically–symmetric growth of a rim of dense product. Two of the new results concerning the rim are essential to understanding the rest of the paper. First, within the rim of dense product, radial deviatoric strain and radial deviatoric strain–rate are of opposite sign: the first is compressive (negative) but the second is tensile (positive). The sign difference is due to the discontinuity in radial strain experienced by a particle as it is transformed. This effect has not been previously recognized. Because of it, strain and strain rate will affect the deviatoric stress and, therefore, the pressure distribution differently. Second, at the phase interface the radial deviatoric strain within the rim is independent of time.

Though previous models of rim growth all assume spherical symmetry, they differ from the present treatment because they introduce a constitutive assumption at the outset. However, if those models were correctly formulated, they should, for the special case of incompressible phases, possess the two properties stated in the preceding paragraph. In the appendix, however, we show the models of Liu et al. (1998), Mosenfelder et al. (2000) and Morris (2002) all predict, incorrectly, that the strain at the phase interfaces develops with time

from an initial value of zero. Those models also predict the wrong sign for the radial deviatoric strain within the rim. Because a correct calculation of strain is necessary to predicting any other property of the model, it is nugatory to apply kinematic incorrect models to experiments, or to the earth.

With these results established, in §3, we analyse growth in a perfectly elastic sphere. After a careful formulation of the constitutive equation, similar to that given by Lee and Tromp (1995), we introduce the kinetic relation. Following Vaughan et al.(1984), and other standard works cited within the text, we take the interface velocity to be determined by the difference in a certain thermodynamic potential across the phase interface. Our use of this standard relation *differs* from that Vaughan et al.(1984) and Green (1987); whereas in their applications, the effect of strain energy on interface velocity could be taken as negligibly small, this is not so here. Indeed, we show that the potential difference driving transformation results from a competition between the strain energy stored in a freshly transformed particle, and the pressure–work performed in reducing the specific volume as the phase interface sweeps across the particle. When the rim is thin, there is a certain range of excess pressure within which the first term dominates the second: growth of a thin rim of dense product is then energetically prohibited because the pressure–work available is less than the strain energy which would be stored if the particle transformed. This effect is manifested as an energy barrier to transformation: in figure 7, the maximum potential occurs when the rim has zero thickness, and only if the excess pressure is sufficiently large is the sign of that maximum such as to allow transformation. According to the elastic model, there is a certain range of excess pressure within which the two phases can not coexist; instead, either phase can exist metastably there. This prediction *differs* from that of Liu et al.(1998); based on their analysis of growth in an elastic solid, they propose that strain energy develops with time, and that rim growth only ceases after a certain amount of transformation (Liu et al. 1998, p.23898).

This prediction of metastability is not consistent with the Kubo et al. (1998a) experiments in which a rim of product coexists with a core of parent phase. We are therefore led to include the effect of plastic deformation. Because it has not been previously recognized that deviatoric strain and deviatoric strain–rate are of opposite sign during rim formation, we have chosen to illustrate the effect of rate–dependence using the simplest constitutive equation for which the sign of the strain–rate affects the deviatoric stress. With this motivation, in §4, we analyse growth in a perfectly plastic solid, that is, without strain hardening. (For brevity, we refer to the corresponding deformation as creep; see the final paragraph of this section for discussion.) We show that, when conditions are such that the rim yields, the strain energy density on the rim side of the phase interface now varies as the square of the yield stress: the smaller the yield stress, the lower is the energy barrier to transformation. In this sense, creep promotes transformation. Creep has, however, a second effect: as a function of volume fraction occupied by the parent phase, the pressure within the parent phase has a minimum (less than the applied pressure). Because the presence of this minimum reduces the pressure–work tending to drive transformation, this effect

of creep tends to inhibit transformation. As a result of these competing effects, the potential difference now has an altogether more interesting shape than that found for elastic phases. According to figure 11, the maximum in $[G]_1^2$ now occurs for non–zero rim thickness. Because we predict that this maximum can be of either sign, it can either cause rim growth to cease (as observed in the Kubo et al.(1998a) experiments, or it can allow complete transformation of the sample, albeit at a time–dependent rate.

With the properties of our model established, we consider two applications. In §5 we discuss the behaviour to be expected from a series of experiments in which the excess pressure is increased quasi–statically, that is on a time scale large compared with permitted by interface kinetics in a sample at uniform pressure. Based on solutions discussed in §4, we argue that, up to a certain critical value of excess pressure depending on the yield stress, rim and sample mean density will increase smoothly with the excess pressure; above that critical excess pressure, however, transformation will occur rapidly compared with the time scale set by the applied pressure. Though this behaviour suggests a model for deep earthquakes, the presence of two time scales in the behaviour implies that the assumption of constant yield stress is unlikely to hold. It will therefore be necessary to extend the present model allowing for a more realistic creep law, along the lines set out by Morris (1995). As a second example, in §6 we use the present solution to estimate yield stresses for the rim phases in the experiments of Kubo et al. (1998a,b) and of du Frane et al.(2013).

The editors of this special volume have asked me to clarify the distinction between plasticity (which they define as flow with finite strength) and creep (which they define as flow with zero strength). My usage of these terms is the same as that of Karato (2008, §9.6). At high stresses, or at sufficiently low temperature, strain rate varies exponentially (and strongly) on stress; conversely, the stress depends only weakly on strain–rate and temperature. The theory of ideal plasticity can be used in this case; it must of course be kept in mind that the yield strength in that model refers to an experiment on a particular time–scale. Though this régime is called 'low–temperature plasticity', it can occur at high temperatures if the stress difference is sufficiently large: see for example Kawazoe et al. (2010). In the experiments of Kubo et al., the stress difference is of the order of the excess pressure times the ratio of sample dimension to rim thickness; it is of the order of a GPa. For this reason, low–temperature plasticity appears to be a reasonable first approximation. Morris (1995, figure 3) shows numerically that when deformation occurs by low–temperature plasticity, the stress field consists of plastic and elastic regions, exactly as predicted by the theory of ideal plasticity.

2. Kinematics of spherically–symmetric deformation

Figure 1 shows the spherical sample of radius b. We assume the densities ρ_1 and ρ_2 of the phases to be uniform in space and time. Because the results in this section are purely kinematic, we do not show material properties or the pressure applied to the outer sample boundary. To make the description as concrete as

possible, we suppose that the parent phase occupies the central sphere, and the product occupies the rim.

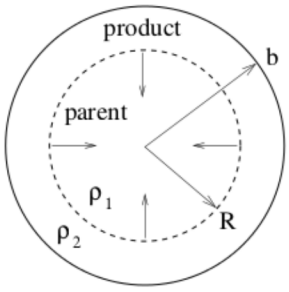

Figure 1: Definition sketch for the kinematic analysis.

2.1. Results holding for arbitrary strains

Although ρ_1 and ρ_2 are constant in space and time, the density of the whole sample increases as the phase interface propagates inwards from its initial location R_0 to its current location R. As a result, the sample contracts: a particle of material that has been transformed moves from its initial location r_0 to its current location r. Because the phases are incompressible, and the motion is spherically–symmetric, r is determined by mass conservation alone.

We show without approximation that r is given as a function of r_0, R_0 and R by the following expression:

$$r^3 = \begin{cases} r_0^3, & 0 < r_0 < R; \\ \frac{\rho_1}{\rho_2} r_0^3 + \frac{\rho_2 - \rho_1}{\rho_2} R^3, & R < r_0 < R_0; \\ r_0^3 - \frac{\rho_2 - \rho_1}{\rho_2}(R_0^3 - R^3), & R_0 < r_0. \end{cases} \qquad (1a, b, c)$$

Case (1a) describes a particle that is initially located at a radius r_0 that is less than the current radius R of the phase interface. Because this particle has not yet been transformed by the inward propagating interface, conservation of mass requires that $4\pi\rho_1 r_0^3/3 = 4\rho_1 \pi r^3/3$. So, $r^3 = r_0^3$ as stated by (1a).

Figure 2 illustrates case (1b). In the initial configuration (figure 2a), the particle initially consists of parent phase. In the current configuration (figure 2b) $R < r_0$: the phase interface has propagated inwards past the initial location r_0 of the particle. Because all particles initially located on a spherical surface of radius r_0 have been transformed, they have moved inwards to radius r. (We recall that a surface consisting of the same particles for all time is said to be a *material surface*.)

The current location r of this material surface r_0 is determined by mass conservation. In the initial configuration, figure 2a, the mass within the surface

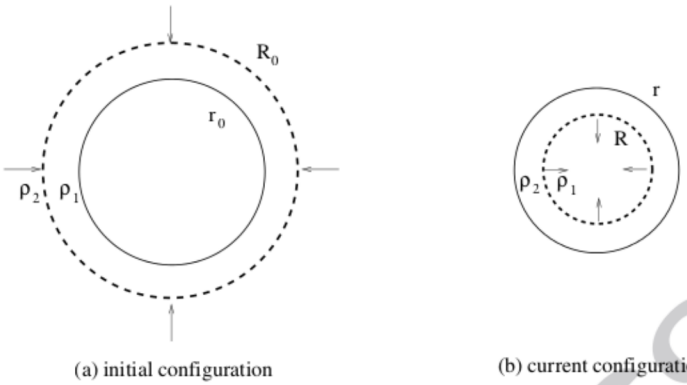

Figure 2: Displacement of a material surface (solid circle) from an initial state in which it had not yet been transformed. The phase interface (broken circle) propagates inwards. (a) Before transformation: the material surface has radius r_0; the interface has radius $R_0 > r_0$. (b) After transformation: the material surface has radius is r; the interface has radius $R < r$.

is given $m = 4\pi\rho_1 r_0^3/3$; in the current configuration, figure 2b, the mass is given by $m = 4\pi\{\rho_2(r^3 - R^3) + \rho_1 R^3\}/3$. Equating these expressions for m, then solving for r^3, we obtain (1b). To show explicitly that the material surface has been transformed, we need only express (1b) in the form $r^3 - R^3 = \rho_1(r_0^3 - R_0^3)/\rho_2$: we now see that $r_0 < R_0$ implies that $r < R$; the particle was initially within the parent phase, but is currently within the product.

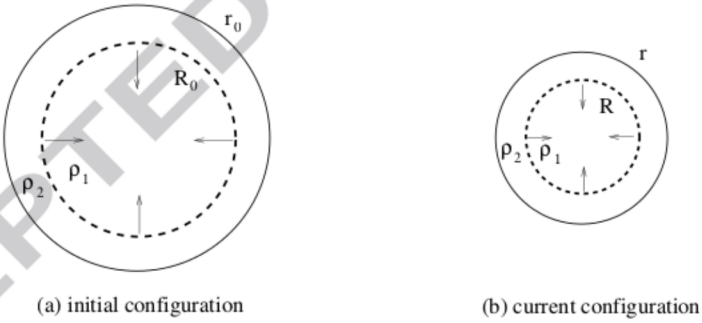

Figure 3: Displacement of a material surface (solid circle) owing to transformation occurring deeper within the sample. In both the initial configuration (a) and current configuration (b), the phase interface (broken circle) lies within the material surface. See text for discussion.

Figure 3 illustrates the final case (1c). In this case, this particle was initially located outside the phase interface (figure 3a); because it consisted of product phase even in the initial state, it does not itself undergo transformation. However, it moves inwards in response to transformation occuring deeper within the

sample. Figure 3b shows the current configuration, in which the phase interface has propagated inwards to its current location R. Mass conservation requires that $\rho_1 R_0^3 + \rho_2({r_0}^3 - R_0^3) = \rho_1 R^3 + \rho_2(r^3 - R^3)$. Rearranging, we obtain (1c). We note that (1c) does *not* hold at the phase interface: expressing (1c) in the form $r^3 - R^3 = r_0^3 - R_0^3 + \rho_1(R_0^3 - R^3)/\rho_2$, and recalling that in this case $R_0 < r_0$, we see that $r^3 > R^3$.

Case (1c) occurs, for example, when an inclusion of one mineral transforms within a matrix consisting of a second mineral not undergoing transformation. Figure 1 of Gillet et al.(1984) shows an inclusion of silica within a garnet matrix; the inclusion comprises a central core of dense coesite phase surrounded by rim of less dense quartz phase. According to Gillet et al., during uplift the rock has been subject to a reduction in applied pressure. As a result, a rim of low–pressure phase (quartz) has formed around the high–pressure phase (coesite). Though the garnet matrix is not transformed, fractures within it radiate away from the silica inclusion, showing that the garnet is strained as a result of the expansion of the silica inclusion. (In equation 1c, we are of course taking the density of the matrix to equal that of the high–pressure phase in the rim.)

In the following, we emphasize the behaviour of the rim of high–pressure product. The results for the matrix are discussed in the Appendix, where they are used to explain the differences between the present work and previous (erroneous) analyses of rim growth.

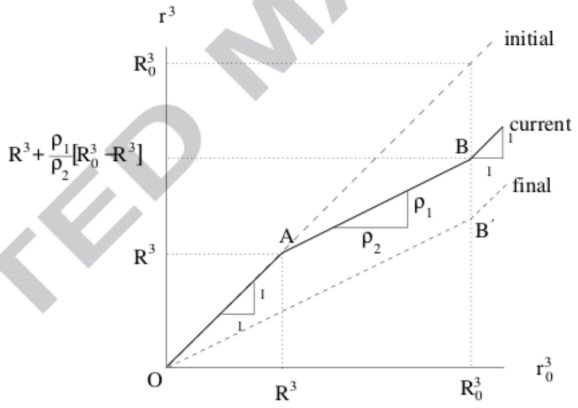

Figure 4: Relation (1) between r^3 and r_0^3. See text for discussion.

Figure 4 shows the entire relation (1). To interpret the figure, we fix the initial radius R_0 of the phase interface, and treat the current radius R as a parameter. Because we are considering an inward growing rim, $R < R_0$. In the initial state $r = r_0$, and the phase interface is at R_0. In the current state, the interface has moved inwards to R and, from the abscissa, we see that all material initially located between R_0 and R has been transformed. In the final state, $R = 0$, and the outermost particle B to have been transformed has moved inwards to

point B'. Because this particle is finally located at radius $r = R_0(\rho_1/\rho_2)^{1/3}$, a spherical sample of initial radius R_0 suffers a (fractional) change in radius equal to $1 - (\rho_1/\rho_2)^{1/3}$. For the olivine–wadsleyite transformation, the percentage change in sample radius is about 2%.

2.2. Specialization to small strains

As a result of the transformation, the material surface has suffered a displacement $u = r - r_0$. Eliminating r_0 between this definition, and equation (1), we obtain u as a function of r, R_0 and R. Though we could do this without approximation, it is more instructive to use the fact that for the transformations of interest $|\rho_2 - \rho_1|/(3\rho_1) \ll 1$. In this case, $|u| \ll r$ and the strain also proves to be small.

For $|u| \ll r$, we may approximate $r_0^3 = (r-u)^3$ in each member of (1) by $r^3 - 3r^2u$. Solving the resulting expressions for u, we obtain

$$u = \begin{cases} 0, & 0 < r < R; \\ -\frac{\rho_2-\rho_1}{3\rho_1}\left(r - \frac{R^3}{r^2}\right), & R < r < r_1; \\ -\frac{\rho_2-\rho_1}{3\rho_2}\frac{R_0^3-R^3}{r^2}, & r_1 < r. \end{cases} \qquad (2a, b, c)$$

Here

$$r_1 = \left[R^3 + \frac{\rho_1}{\rho_2}(R_0^3 - R^3)\right]^{1/3}. \qquad (3)$$

(Equation (3) is obtained from the ordinate of point B in figure 2.) Unlike the phase interface, the interface at $r = r_1$ is material. It separates matter which had density ρ_2 in the initial state, and which is not transformed, from matter that has been transformed.

We note the following properties of (2). First, at each interface, the displacement u is continuous; no gaps open within the material. In particular, at the phase interface $r = R$, $u(R) = 0$. (A reviewer has suggested that gaps (pores) might open if the strain is tensile. During growth of an isolated sphere of dense high–pressure phase, the radial deviatoric strain is indeed tensile in the surrounding parent phase (Morris 1992, eq.5). But, if a gap *were* to open anywhere, the pressure within it would fall to the vapour pressure of the solid. The high–pressure phase would then revert to the low–pressure phase, and transformation would be impossible. For this reason, I believe that transformation to a high–pressure phase proceeds at the rate permitted by the condition of material continuity.)

Second, according to (2)

$$\operatorname{div}\mathbf{u} = \begin{cases} 0, & 0 < r < R; \\ -\frac{\rho_2-\rho_1}{\rho_1} & R < r < r_1; \\ 0, & r_1 < r. \end{cases} \qquad (4a, b, c)$$

(The displacement vector $\mathbf{u} = u(r)\mathbf{e}_r$.) From (4b), we see that within the product, div $\mathbf{u} \neq 0$. Although each phase is incompressible, an element of material changes its volume when it is transformed.

Equation (4) is, of course, consistent with the theory of infinitesimal strain. As described by Love (1927, §25), if as a result of deformation, the volume of an element of material changes from V_0 in the undeformed state to V in the deformed state, the divergence of the displacement vector for that element is equal to the ratio $(V - V_0)/V_0$. In our case, the volume of unit mass of material within the rim has changed from its initial value $V_1 = \rho_1^{-1}$ before transformation to its final value $V_2 = \rho_2^{-1}$ after transformation. Consequently,

$$\frac{V - V_0}{V_0} = \frac{V_2 - V_1}{V_1}, = \theta_T. \qquad (5a, b)$$

Because we are assuming that the fractional difference in specific volume is small, $|\theta_T| \ll 1$, we may replace ρ_1 in the denominator of (4b) by ρ_2; we obtain div $\mathbf{u} = \theta_T$. It follows that (4b) is consistent with the general result given by Love. (For a rim of dense phase, $\theta_T < 0$.)

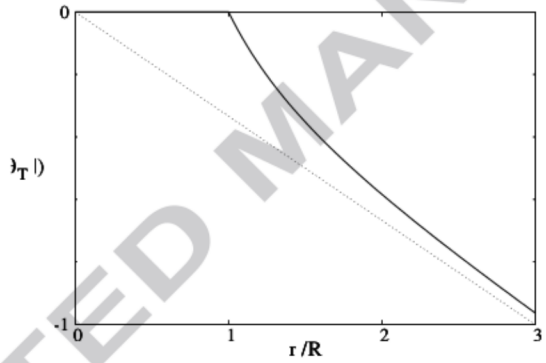

Figure 5: Displacement caused by growth of a dense product rim. Solid curve, equations (2a) and (2b); broken line, asymptote for $r/R \gg 1$. As defined by (5), $\theta_T = (V_2 - V_1)/V_1$. See text for discussion.

Figure 5 shows the displacement field (2). To emphasize the behaviour near the phase interface, we do not include case (2c). To interpret the figure, let us consider an experiment in which a thin rim of dense product nucleates on the surface of the spherical sample. Because the rim initially has negligible thickness, all material within it is initially close to the phase interface; because $r \to R$, initially $u \to 0$. Because R decreases as the phase interface propagates inwards, r/R increases at any fixed location r. Asymptotically, as $R \to 0$, $r/R \to \infty$, and the displacement approaches the asymptote

$$u = \tfrac{1}{3} r \theta_T,$$

indicated by the broken line. This asymptote describes the final isotropic contraction of the sample resulting from the transformation. In figure 4, this asymptote corresponds to final line OB'.

Because the sample contracts as a result of its transformation, the radial strain is plainly negative (compressive). Moreover, within the product rim, the radial *deviatoric* strain is also negative: indeed, from figure 5, we see that the slope of the curve $u(r)$ is more negative than that of its large–r asymptote representing the isotropic contraction. This effect is a consequence of the constraint $u(R) = 0$.

For this spherically–symmetric deformation, the non–zero components of the deviatoric strain tensor in spherical polar coordinates $\{r, \theta, \phi\}$ are given by

$$e'_{rr} = \tfrac{2}{3} r \frac{\mathrm{d}}{\mathrm{d}r}\Big(\frac{u}{r}\Big),$$

and $e'_{\theta\theta} = e'_{\phi\phi} = -\frac{1}{2} e'_{rr}$. Substituting for u from (2), we find that

$$e'_{rr} = \begin{cases} 0, & 0 < r < R; \\ \frac{2}{3}\theta_T \frac{R^3}{r^3}, & R < r < r_1; \\ -\frac{2}{3}\theta_T \frac{R_0^3 - R^3}{r^3}, & r_1 < r. \end{cases} \qquad (6a, b, c)$$

Two implications of (6) are essential to understanding growth of a product rim. First, evaluating (6b) at the phase interface at $r = R$, we find that the radial deviatoric strain is equal to $\frac{2}{3}\theta_T$. No matter how far the phase interface has propagated, every unit mass of product immediately within the rim has been strained by exactly the same amount. For a rim of dense product, this strain is negative (compressive) because $\theta_T < 0$. For the olivine–wadsleyite transformation $|\theta_T| = 0.06$ (Mosenfelder et al. 2001, §2.3), so that a freshly transformed particle within the rim has undergone a *deviatoric* radial strain of 4%, no matter how far the interface has propagated. As a result, deformation is unlikely to be purely elastic, even in the very earliest stages of growth; if deformation were elastic, the corresponding deviatoric radial stress $2\mu e'_{rr}$ would exceed 8 GPa for the rigidity $\mu = 110$ GPa appropriate to wadsleyite (15 GPa, 1500 K). For their series at 13.5 GPa and 1303 K, Kubo et al. describe the dislocation textures after 600 minutes; I think it would be interesting to see the development of those textures, starting at much earlier times.

The magnitude of the radial deviatoric strain is also significant because it controls the development of the dislocation structures allowing plastic deformation; see for example Kawazoe et al.(2010, fig.7).

Second, evaluating (6b) at a fixed value of r within the rim, we see that the magnitude of the radial deviatoric strain decreases in time as $R \to 0$. Because that strain is compressive within a rim of dense product, the corresponding deviatoric strain *rate* is positive (tensile). Within the product rim, the strain and the strain rate are therefore of opposite sign. As a result, even the *sign* of

the pressure difference across the rim depends on the constitutive relation for the product. This effect is illustrated by the examples in §3 and §4.

Because understanding the radial deviatoric strain at the interface is so important for the mechanics of transformation, we show that the previous results can be derived without using the details of the displacement field. For spherically–symmetric deformation, the radial deviatoric strain is related to div $\mathbf{u}$ and u by the following identity:

$$e'_{rr} = \tfrac{2}{3}\mathrm{div}\,\mathbf{u} - \frac{2u}{r}. \tag{7}$$

Because the phases are incompressible, the central sphere is not deformed; as a result, at $r = R$ the displacement $u = 0$ because u is continuous across the interface. Further, throughout the rim, div $\mathbf{u}$= θ_T, by the argument used to interpret (4b). Substituting these expressions into (7), we find that at $r = R$

$$e'_{rr} = \tfrac{2}{3}\theta_T. \tag{8}$$

This agrees with (6b). We note that the radial deviatoric strain at fixed r is a discontinuous function of time: within the core of parent phase ($r < R$), $e'_{rr} = 0$ whereas $e'_{rr} \neq 0$ on the product side $r > R$ of the interface. In the appendix, this result is used to explain the major difference between the present analysis and existing analyses of the Kubo et al. experiments.

In the next two sections, we work out two examples to show the implications of these kinematic results.

3. Rim growth in an elastic sphere

Figure 6 shows the geometry of the model. The rim of product has rigidity (shear modulus) μ. In the reference state (initial state), the sample is at uniform hydrostatic pressure equal to the applied pressure p_a: in this state, for $0 \leq r < b$, the stress tensor $\sigma_{ij} = -p_a\delta_{ij}$, where δ_{ij} denotes the unit tensor. We use the convention usual in mechanics and in seismology, in which tensile stresses are taken as positive. We assume the temperature T to be uniform in space and in time.

We assume that the applied pressure p_a is independent of time, so that the volume of the whole sphere can adjust freely as the mean density of the sample changes as a result of the transformation. For the Kubo et al. experiments this assumption appears to be appropriate because the bulk modulus of the pressure medium (halite) is relatively low, about one fifth that of olivine. Even if the anvil itself acted as a rigid container, the volume change in the sample can be accomodated by a relatively small change in the pressure within the halite.

To pose the constitutive equation, we must distinguish between the thermodynamic state of a given phase, and the path by which this state is achieved in a particular experiment. In our case, product is generated as the phase interface propagates across the sample. As a unit mass is transformed, its volume

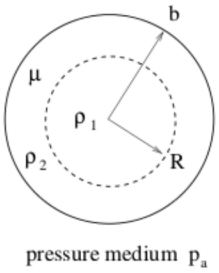

Figure 6: Growth of a product rim in an elastic sphere.

changes; we have shown that within the product, the divergence of the displacement vector is consequently non–zero, even though each phase is incompressible. However, if a small cube of product were removed, without additional deformation, an observer ignorant of its history would only be able to measure the strain existing within the product itself. As far the observer is concerned, the product could equally have been formed by transformation of a low–pressure phase, or by epitaxial deposition from a vapour.

We conclude that, within the product, the state of stress within a particle of incompressible material can only depend on the difference e'_{ij} between the total strain e_{ij} suffered by that particle during growth, and the (constant) dilatational strain tensor e^{T}_{ij} defining the difference between the two phases. According to our discussion of (4),

$$e^{\mathrm{T}}_{ij} = \tfrac{1}{3}\theta_T \delta_{ij}. \tag{9}$$

This uniform strain corresponds to the 'free' or 'stress–free' strain described by Lee and Tromp (1995).

Within the incompressible product therefore

$$\sigma_{ij} = -p\delta_{ij} + 2\mu e'_{ij}, \tag{10a}$$

where

$$e'_{ij} = \tfrac{1}{2}\Big(\frac{\partial u_i}{\partial x_j} + \frac{\partial u_j}{\partial x_i}\Big) - e^{\mathrm{T}}_{ij}. \tag{10b}$$

Within the incompressible parent phase, the deviatoric strain vanishes by(6a), and the stress tensor is isotropic:

$$\sigma_{ij} = -p\delta_{ij}. \tag{10c}$$

3.1. Pressures

Because according to (4), div $\mathbf{u}$ is uniform within each phase, we find on substituting (2) into the Cauchy condition of equilibrium that $\mathbf{u}$ satisfies the usual Navier–Cauchy equations for an incompressible solid: within each phase,

$$\nabla p = -\mu \nabla \times (\nabla \times \mathbf{u}). \tag{11}$$

For the spherically–symmetric solution, the displacement vector is given by $\mathbf{u} = u(r)\mathbf{e}_r$, so that curl $\mathbf{u}$=0. Within each phase, p is therefore uniform.

Let p_1 be the pressure within the central sphere and p_2, that within the rim. Imposing the condition that the normal stress be continuous at $r = R$, we obtain

$$-p_1 = -p_2 + 2\mu e'_{rr}(R^+); \tag{12a}$$

similarly, at $r = b$

$$-p_2 + 2\mu e'_{rr}(b^-) = -p_a. \tag{12b}$$

As shown in figure 6, p_a is the pressure applied to the sample surface by the pressure medium.

Eliminating p_2 between (12a) and (12b), then substituting for e'_{rr} from (6), we obtain

$$p_1 - p_a = -\tfrac{4}{3}\mu\theta_T(1 - f), \tag{13a}$$

$$f = R^3/b^3 \tag{13b}$$

denotes the volume fraction of parent phase. Because $\theta_T < 0$ for a rim of dense product, the pressure p_1 within the inclusion of less–dense parent phase *exceeds* the applied pressure. This is a consequence of the compressional strain within the rim of dense product.

For later use, we note the expression giving the work done on unit mass of parent phase with specific volume V_1 as it is transformed into product with specific volume V_2:

$$(p_1 - p_a)(V_1 - V_2) = \tfrac{4}{3}\mu V_1\theta_T^2(1 - f). \tag{14}$$

(In the form $\sigma_{rr} = -p_1$, we have used the continuity of the normal stress across across the phase interface. We note that, because the deformation is spherically–symmetric, no shear work is performed.)

3.2. Kinetic equation

The kinetics of incoherent transformation are formulated by Vaughan et al.(1984). According to their (3c), for small departures from equilibrium, mass is converted from phase 1 to phase 2 at a rate proportional to the difference $[G]_1^2$ in the values taken by the thermodynamic potential G (per unit mass) on either side of the phase interface:

$$\frac{\mathrm{d}R}{\mathrm{d}t} = \lambda[G]_1^2. \tag{15}$$

Because G has dimensions of energy per unit mass, the kinetic constant λ has dimensions of inverse velocity. (The linearization in (15) is appropriate if the potential difference (per mole) is small compared with the product R_mT of the molar gas constant with the absolute temperature. When we discuss the experiments in §6, the linearization is not an issue because we consider only cases in which the rim has ceased to grow; for those cases, $[G]_1^2 = 0$.)

The potential G is, for the spherically–symmetric geometry shown in figure 6 (above), given in terms of the Helmholtz free energy F per unit mass and specific volume $V = \rho^{-1}$ by $G = F - V\sigma_{rr}$. (We may note that, because Vaughan et al. use a sign convention in which compressive stresses are taken as positive, in their equation (2a) the sign of the coefficient of σ_{rr} is opposite to that given here.) For our case, the stress within the central sphere is purely hydrostatic, $\sigma_{ij} = -p_1\delta_{ij}$ and, moreover, σ_{rr} is continuous across the phase interface. The potential can therefore be expressed as $G = F + p_1 V$. Here, G, F and V are evaluated for phase 1 or phase 2 as appropriate, but p_1 is (always) the pressure within the central sphere. In this form, the potential is, of course, identical with that derived by Gibbs (1928, equation 372) in his discussion of the equilibrium of an elastic solid with a liquid; see also Paterson (1973, equation 7).

To interpret the potential, we note that

$$[G]_1^2 = F_2 - F_1 + p_1(V_2 - V_1) : \tag{16}$$

when unit mass is transformed from phase 1 to phase 2, the change $G_2 - G_1$ in its potential is equal to the difference between the change $F_2 - F_1$ in its strain (Helmholtz) energy and the pressure–work $p_1(V_1 - V_2)$ performed upon it. Based on this interpretation, we expect that when the pressure–work exceeds the change $F_2 - F_1$ in stored strain energy, phase 2 will grow at the expense of phase 1.

This expectation is consistent with (15). According to Heidug & Lehner (1985), the second law of thermodynamics requires the kinetic constant λ to be non–negative. From (15), we see that when the rim phase 2 has lower potential at the interface than phase 1, so that $G_2 < G_1$, the interface propagates into phase 1. The effect is to increase the mass of phase having the lower value of G. This is consistent with our interpretation of (16).

The physical interpretation given in the preceding paragraphs is illustrated by the examples given later: see, for example, the discussion of (24).

Let $\bar{p}$ be the Clapeyron pressure at which the phases coexist at common pressure, and let $[\bar{F}]_1^2$ be the difference between the Helmholtz free energies in this hydrostatic state. Because, in this state, the phases are in equilibrium, the right hand side of (15) vanishes: $0 = [\bar{F}]_1^2 + \bar{p}[V]_1^2$. Subtracting this expression from (16), we obtain

$$[G]_1^2 = [F - \bar{F}]_1^2 + (p_1 - \bar{p})[V]_1^2. \tag{17}$$

Because no constitutive assumption has yet been made, (17) gives the difference $G_2 - G_1$ for two phases of an arbitrary material. This relation holds for spherically–symmetric deformation of incompressible phases provided σ_{rr} is continuous at the phase interface; the latter assumption is valid for the Kubo et al. experiments because surface tension is negligibly small. Because no constitutive assumption has been made, the expressions in section hold equally if the deformation is elastic, or plastic. Using them, we now complete our discussion of rim growth in an elastic solid.

3.3. Helmholtz function

According to the Gibbs identity, in an isothermal process, an increment $\mathrm{d}e_{ij}$ in strain increases the Helmholtz function F of an incompressible phase by

$$\mathrm{d}F = V\sigma_{ij}\mathrm{d}e'_{ij}. \tag{18}$$

Here, and in the rest of this work, V denotes the mean specific volume of the phases: $V = \frac{1}{2}(V_1 + V_2)$.

Substituting Hooke's law (10) into (18), then simplifying, we obtain

$$\mathrm{d}F = V\mu\mathrm{d}(e'_{ij})^2, = \tfrac{3}{2}V\mu\mathrm{d}(e'_{rr})^2. \tag{19a,b}$$

We have used the relations $e'_{\theta\theta} = e'_{\phi\phi} = -\frac{1}{2}e'_{rr}$.

Let F_0 be the value of F in the initial state, in which $\sigma_{ij} = -p_a\delta_{ij}$. Integrating (19b) from the initial state to the current state, we find that

$$F - F_0 = \tfrac{3}{2}V\mu(e'_{rr})^2. \tag{20}$$

Using (8) to evaluate (20) for the product phase in its state of strain on the outer side of the interface, we obtain

$$F_2 = F_{02} + \tfrac{2}{3}\mu V\theta_T^2. \tag{21a}$$

For the parent phase on the inner side of the interface,

$$F_1 = F_{01}. \tag{21b}$$

In (21b), there is no contribution from the strain energy because within the central sphere, the stress is hydrostatic, and the phases are incompressible.

Subtracting (21b) from (21a), we obtain

$$[F]_1^2 = [F_0]_1^2 + \tfrac{2}{3}\mu V\theta_T^2. \tag{22}$$

Because the phases are incompressible, the difference in the Helmholtz free energies is the same for any two states of hydrostatic stress; so $[\bar{F}]_1^2 = [F_0]_1^2$. Subtracting this expression from (22), we obtain

$$[F - \bar{F}]_1^2 = \tfrac{2}{3}\mu V\theta_T^2. \tag{23}$$

According to (23), the difference between the values of strain energy per unit mass on either side of the interface is invariant in time. No matter how far (or how little) the interface has propagated, every unit mass suffers the same in strain energy when it is transformed.

3.4. Discussion of the potential difference

Expressing (17) in the form

$$[G]_1^2 = [F - \bar{F}]_1^2 + \big\{(p_1 - p_a) + (p_a - \bar{p})\big\}V\theta_T, \tag{17′}$$

then using (14) and (23), we find that

$$[G]_1^2 = V\big\{(p_a - \bar{p})\theta_T + \tfrac{4}{3}\mu\theta_T^2(f - \tfrac{1}{2})\big\}. \tag{24}$$

As defined by (13b), f denotes the volume fraction occupied by the central sphere.

This formula illustrates the physical interpretation of $[G]_1^2$ given in §3.2. On the right hand side of (24), the first term represents the potential difference that would exist if the sample were at uniform pressure p_a. Because, for a rim of dense phase, this term is negative for $p_a > \bar{p}$. it represents an energy source for transformation. The second term represents the net effect of deviatoric stress within the rim. The change in the sign of this term at $f = 1/2$ illustrates the discussion in §3.2: according to (23), the strain energy density at the interface is independent of f, whereas from (14), we see that the pressure work becomes increasingly large as f decreases. For $f > 1/2$, the strain energy dominates the pressure–work, so that $[G]_1^2 > 0$; in this range of f, deviatoric stress inhibits transformation. Conversely, for $f < 1/2$ the pressure–work exceeds the strain energy stored; as a result, deviatoric stress now promotes transformation.

We define the pressure ratio Π as follows:

$$\Pi = -(p_a - \bar{p})/\big(\tfrac{4}{3}\mu\theta_T\big). \tag{25}$$

For a rim of dense product $\theta_T < 0$, so that $\Pi > 0$ if the applied pressure pressure p_a exceeds the coexistence pressure $\bar{p}$. In this notation, (24) becomes

$$[G]_1^2 = \tfrac{4}{3}\mu V\theta_T^2\big\{f - \tfrac{1}{2} - \Pi\big\}. \tag{26}$$

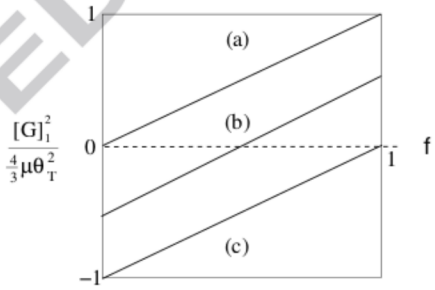

Figure 7: Potential difference $[G]_1^2$ for elastic phases as a function of volume fraction $f = R^3/b^3$. Case (a), $\Pi = -\frac{1}{2}$, i.e. $p_a = \bar{p} - \frac{2}{3}\mu|\theta_T|$. Case (b), $\Pi = 0$, $p_a = \bar{p}$. Case (c), $\Pi = \frac{1}{2}$, i.e. $p_a = \bar{p} + \frac{2}{3}\mu|\theta_T|$. See text for discussion.

Figure 7 shows the relation (26); in the $\{f, [G]_1^2\}$ plane, the equation represents a family of parallel lines having unit slope, and intercept depending on the excess pressure $p_a - \bar{p}$. Because for a rim of dense product, the parameter $\theta_T < 0$, case (a) corresponds to applied pressure p_a lower than the coexistence pressure

$\bar{p}$ by $\frac{2}{3}\mu|\theta_T|$; case (b) corresponds to $p_a = \bar{p}$; and case (c), to p_a exceeding $\bar{p}$ by $\frac{2}{3}\mu|\theta_T|$.

According to the figure, the maximum value of the potential difference $[G]_1^2$ always occurs at $f = 1$, that is, for a product rim of negligibly small thickness. (The physical reason for this maximum is discussed in the paragraph following equation 24.) Because the kinetic relation (15) requires that $[G]_1^2$ be negative for the low–pressure phase 1 within the core to transform to the high–pressure phase, positive values of $[G]_1^2$ represent an energy barrier to product formation. In case (a), $[G]_1^2 > 0$ for all volume fractions: the excess pressure is too low for any amount of dense phase to exist. In case (b), $[G]_1^2 < 0$ for core fraction $f < 1/2$; the pressure–work tending to drive transformation can then overcome the fixed cost of storing energy within the rim. Though transformation *could* proceed *if* a product rim occupying half the sample volume were (somehow) able to nucleate, the positive values of $[G]_1^2$ for $\frac{1}{2} < f < 1$ represent an energetic barrier to growth of any thin rim of product nucleating on the sample outer boundary. Lastly, in case (c), the excess pressure is sufficiently large that $[G]_1^2 < 0$ for all $f < 1$; in this case, an arbitrarily thin rim of dense product that nucleates on the sample boundary can grow into the sample, and transform it completely. Without modification, figure 7 also describes the energetic barrier to growth of a central sphere of less dense product. In this case, of course, for a dense rim to transform into the less dense core phase, $[G]_1^2$ must be positive. We see that, over the same pressure range, an energetic barrier also prevents growth of a central sphere of less dense product.

We conclude that, in an elastic solid having incompressible phases, transformation in either direction is energetically prohibited if the pressure ratio Π satisfies the condition

$$|\Pi| < \tfrac{1}{2}. \tag{27}$$

We note the related result of Truskinovskiy (1984): specializing his equation (6) to incompressible phases, we see that, according to the Truskinovskiy analysis, formation of an isolated sphere of low density product within an infinite medium is possible only if p_a is less than $\bar{p} - \frac{2}{3}\mu|\theta_T|$. (The Truskinovskiy results overlap with ours only in the case $f \to 0$ describing an isolated sphere; his results for larger values of f describe growth in a spherical sample having *fixed* overall volume. We, of course, have assumed instead that the applied pressure is fixed.)

This picture differs altogether from that proposed by Rubie & Thompson (1985), and subsequently modelled by Liu et al.(1998), and others. By comparing their model with experiment, Liu et al. conclude (p.23898) that 'elastic strain energy develops as the rim grows.... This strain energy, if not dissipated by viscoelastic relaxation (plastic flow), can effectively inhibit growth *after a certain degree of transformation*' (my emphasis). Here, by contrast, we have shown that when the strains are calculated correctly, and the correct form is used for the potential difference entering into the kinetic equation, the elastic model predicts that a finite energy barrier prevents *any* transformation for excess pressures lying within the range given by (27). Evidently, we need another explanation for the observations of Kubo et al.(1998a). We now work out a

second example showing the effect of creep.

4. Perfect plasticity

Figure 8 shows the geometry of the model. As in the previous sections, we take the solid to be isotropic, and the deformation to be spherically symmetric. Owing to this symmetry, the principal stresses are given by $\sigma_{rr} = -p+\sigma'_{rr}, \sigma_{\theta\theta} = \sigma_{\phi\phi} = -p - \frac{1}{2}\sigma'_{rr}$. Specializing the von Mises yield criterion to this stress field, we find that the solid yields when $(\sigma'_{rr})^2 = k^2$, where the material constant $k > 0$. Within the plastic region, σ'_{rr} is therefore related to the radial deviatoric strain rate $\dot{\gamma}$ by

$$\sigma'_{rr} = k \operatorname{sgn} \dot{\gamma}. \tag{28}$$

The factor $\operatorname{sgn}\dot{\gamma}$ is necessary to ensure that the dissipation–rate is non–negative. This factor introduces the following essential feature into the analysis.

Because the strain is small, the strain–rate within the product rim can be obtained by differentiating the expression (6b) for radial strain with respect to t (fixed r):

$$\dot{\gamma} = 2\theta_T \frac{\mathrm{d}R}{\mathrm{d}t}\frac{R^2}{r^3}$$

(Morris 2002, p.1370). We see that $\dot{\gamma} > 0$ for a growing rim of dense product. Because the strain–rate and the strain are of opposite sign, the strain–rate dependence represented by the factor $\operatorname{sgn}\dot{\gamma}$ in (28) changes the sign of the radial deviatoric stress. As a result, transformation proves to be possible once creep is taken into account, provided the plastic region is sufficiently large.

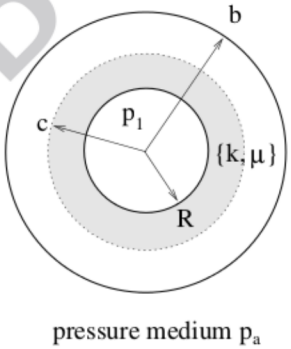

Figure 8: Product rim $R < r < b$ subject to internal pressure p_1 and external pressure p_a; yield surface is of radius c. The plastic region is shaded.

4.1. Thermodynamics

Because the expressions given for strain in §2 are purely kinematic, they are still applicable. In particular, the radial deviatoric strain within the freshly

transformed product is given by (8). Growth in a plastic solid differs, however, from growth in a Hookean solid: now, only part of that kinematically imposed strain is associated with reversible work. This reversible work is stored as internal energy (strain energy) within the phases, and we need to calculate the corresponding Helmholtz free energy to model the propagating phase interface.

Specializing equation (11) of Hill (1967) to our case of an incompressible material, we find that the increment of the part of the strain $\mathrm{d}e^e_{ij}$ associated with reversible work is related to the increment in deviatoric stress by Hooke's law:

$$\mathrm{d}e^e_{ij} = \frac{\mathrm{d}\sigma'_{ij}}{2\mu}. \tag{29}$$

Because the differential is exact, the elastic strain defined by (29) depends only on the current state of stress, and on the reference state; because, by its definition, e^e_{ij} is a state variable, the corresponding Helmholtz free energy is given by the Gibbs identity (17) with e'_{ij} replaced by the elastic strain e^e_{ij}.

Applying (29) to the product phase within the rim, we integrate from the reference state (§3,¶1), in which the deviatoric stress is zero, to the state existing at $r = R+$; in this state, $\sigma'_{rr} = k > 0$ because the radial deviatoric strain–rate is positive. For the radial component of (29), we obtain

$$e^e_{rr} = \frac{k}{2\mu}, \tag{30}$$

$e^e_{\theta\theta} = e^e_{\phi\phi} = -\frac{k}{4\mu}$, similarly. Because $\sigma'_{rr} = k$ throughout the plastic region, the element of material suffers no further change in elastic strain until it leaves this region. We note that although, according to (6b) the radial deviatoric strain is negative (compressive), the elastic strain within the plastic region is positive (tensile). This is a consequence of the strain–rate dependence represented by the factor $\operatorname{sgn}\dot{\gamma}$ in the flow law (28).

The Helmholtz free energy is given by (20), with e'_{rr} replaced by (30):

$$F_2 = F_{02} + \tfrac{3}{8}V\frac{k^2}{\mu}. \tag{31}$$

Substituting (31) and (21b) into (17), we find that

$$[F - \bar{F}]^2_1 = \tfrac{3}{8}V\frac{k^2}{\mu}. \tag{32}$$

(We have used the identity $[F_0]^2_1 = [\bar{F}]^2_1$.) Comparing (32) with the corresponding expression (23) holding for elastic phases, we see that for $k < \frac{4}{3}\mu|\theta_T|$, creep reduces the Helmholtz free energy difference. As we have discussed below (17), storage of potential energy within the rim impedes transformation: by reducing the amount of energy stored, creep promotes transformation.

Substituting (32) into (17), we find that the potential difference driving interface propagation is given by

$$[G]^2_1 = \big\{(p_1 - \bar{p})\theta_T + \tfrac{3}{8}\frac{k^2}{\mu}\big\}V. \tag{33}$$

To evaluate (33), we need the pressure p_1 within the core of parent phase.

4.2. Pressure within the core

The radial stress σ_{rr} and deviatoric radial stress σ'_{rr} are determined as functions of r and the radius c of the yield surface by the following equations: for $R < r < b$,

$$\frac{\mathrm{d}\sigma_{rr}}{\mathrm{d}r} + 3\frac{\sigma'_{rr}}{r} = 0; \tag{34a}$$

$$\sigma'_{rr} = \begin{cases} k \operatorname{sgn} \dot{\gamma} & \text{if } r < c \\ \sigma_{rr} + p_2(t) & \text{if } r > c \end{cases}. \tag{34b}$$

$$\text{At } r = c,\ [\sigma_{rr}] = 0,\ \ (\sigma'_{rr})^2 = k^2; \tag{34c,d}$$

$$\text{at } r = b,\ \sigma_{rr} = -p_a; \tag{34e}$$

$$\text{at } r = R,\ \sigma_{rr} = -p_1. \tag{34f}$$

As (34a), the condition of mechanical equilibrium provides one equation in two unknowns σ_{rr} and σ'_{rr}. The constitutive equation (34b) provides the second relation between these unknowns; within the plastic region, σ'_{rr} satisfies the yield criterion, and within the elastic region the pressure is spatially uniform. Equations (34c) and (34d) connect the solutions in these two regions: at the yield surface $r = c$, the normal stress σ_{rr} must be continuous and the deviatoric stress within the elastic region must satisfy the yield condition. Lastly, (34e) and (34f) express the condition of continuity of normal stress at the sample boundary $r = b$ and at the phase interface $r = R$: $p_1(t)$ is the pressure within the central sphere.

Because σ_{rr} is continuous across the yield surface, we may integrate the equilibrium condition (34a) from $r = R$ to $r = b$, then apply boundary conditions (34e) and (34f). We obtain

$$p_1 - p_a = -3\int_R^b \sigma'_{rr}\frac{\mathrm{d}r}{r}. \tag{35}$$

To evaluate (35), we must consider separately the contributions made by the plastic region and the elastic region.

The radial deviatoric stress is negative (compressive) within the elastic region, but is positive (tensile) within the plastic region:

$$\sigma'_{rr} = \begin{cases} k & \text{for } R < r < c, \\ \frac{4}{3}\mu\theta_T\frac{R^3}{r^3} & \text{for } c < r < b. \end{cases} \tag{36a,b}$$

(We recall that $k > 0$, and that $\theta_T < 0$.) Within the plastic region, $\sigma'_{rr} > 0$ because, according to (9), $\dot{\gamma} > 0$ within a growing rim of dense product. Within the elastic region, the radial deviatoric stress is compressive by (6b) and Hooke's law (10). Within the elastic region, σ'_{rr} decreases with increasing r and, from (36b), we see that if $\frac{4}{3}\mu\theta_T < k$, the maximum value of σ'_{rr} occurring in the transformation is too small to cause yielding.

Let

$$\kappa = \tfrac{3}{4}\frac{k}{\mu|\theta_T|}; \tag{37}$$

for $\kappa > 1$, deformation is purely elastic throughout the rim. (We note that the stress difference $|\sigma_{rr} - \sigma_{\theta\theta}| = 2\kappa\mu|\theta_T|$.)

Imposing the yield criterion (34d) on (36), we find that the radius c of the yield surface is given by

$$c^3 = \kappa^{-1}R^3. \tag{38}$$

Together, (36) and (38) determine the radial deviatoric stress.

We see that, for $\kappa < 1$, there are two cases depending on the relation between κ and the volume fraction f occupied by the central sphere. Because the sample initially consists of only low–pressure phase, volume fractions satisfying $1 > f > \kappa$ correspond to the initial stage of transformation. During it, the radius of the yield surface exceeds the sample radius, and the entire product rim deforms plastically. As transformation proceeds, the product rim becomes sufficiently thick for the deviatoric stress to fall below the yield stress; according to (38), this first occurs when $f = \kappa$. For $f < \kappa$, the yield surface lies within the rim, and the outer part of the rim then deforms elastically.

Figure 9 shows the relation (36) for $\theta_T < 0$, and $f < \kappa < 1$: within the elastic region $r > c$, the radial deviatoric stress is negative because the radial strain is negative; at the yield surface, the magnitude of $\sigma'_{rr} = k$, but the *sign* of σ'_{rr} changes from negative on the elastic side of the yield surface to positive on the plastic side because the strain–*rate* is positive throughout the rim.

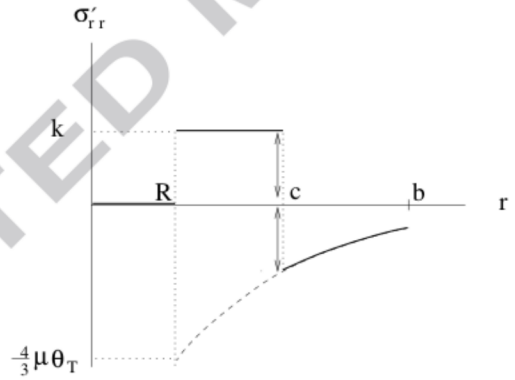

Figure 9: Radial distribution (36) of deviatoric stress σ^0_{rr} for $\theta_T < 0$ (dense product rim), and $f < \kappa < 1$. As discussed in the text, within the rim of product, σ^0_{rr} is tensile (positive) within the plastic region $R < r < c$, but is compressive (negative) within the elastic region $c < r < b$. Within the central sphere $r < R$ of parent phase, the stress is isotropic: $\sigma^0_{rr} = 0$.

Using (36) to evaluate (35), we find that for $\kappa < 1$

$$\frac{p_1 - p_a}{k} = \begin{cases} 1 + \ln\kappa - f/\kappa, & f < \kappa; \\ \ln f, & \kappa < f. \end{cases} \tag{39a,b}$$

For $\kappa = 1$, the entire rim deforms elastically and (39a) is then equivalent to equation (13) of the elastic analysis.

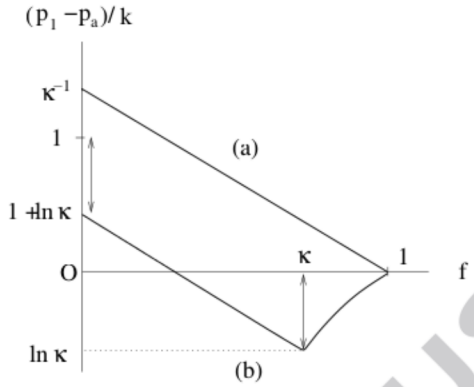

Figure 10: Effect of plasticity on the difference $p_1 - p_a$ between the pressure in the central sphere and that applied at the outer sample boundary. (a) $\kappa \geq 1$, equation (13) describing purely elastic deformation; (b) $\kappa < 1$, equation (39) describing elastic–plastic deformation. See text for discussion.

Figure 10 shows $p_1 - p_a$ as a function of volume fraction $f = R^3/b^3$ for $\theta_T < 0$. For $\kappa > 1$, the deformation is purely elastic; according to curve (a), $p_1 - p_a$ is then positive, and increases monotonically as f is reduced. Curve (b) shows the behaviour for the case $\kappa < 1$, in which part or all of the rim deforms plastically. We see that $p_1 - p_a$ no longer varies monotonically with f. Instead, as f is decreased from unity, p_1 decreases until $f = \kappa$, then increases with further reduction in f. Because the pressure–work driving transformation is an increasing function of p_1, this non–monotonic behaviour is significant for the course of the transformation, as we now discuss.

4.3. Potential difference

For $\kappa < 1$, the rim yields so that $p_1 - p_a$ is given by (39). Using that result, and the identity $p_1 - \bar{p} = (p_1 - p_a) + (p_a - \bar{p})$, we express (33) in the form

$$\frac{[G]_1^2}{\frac{4}{3}\mu V \theta_T^2} = \begin{cases} f + \frac{1}{2}\kappa^2 - \kappa(\ln\kappa + 1) - \Pi, & f < \kappa; \\ -\kappa \ln f + \frac{1}{2}\kappa^2 - \Pi, & \kappa < f. \end{cases} \qquad (40a, b)$$

As defined by (25), the pressure ratio $\Pi = -(p_a - \bar{p})/\frac{4}{3}\mu\theta_T$. For $\kappa > 1$, deformation is purely elastic, and $[G]_1^2$ is then given by (26).

Two properties of (40) are important for understanding the transformation. The first is the sign of $[G]_1^2$ at $f = 1$: for any product to form, $[G]_1^2$ must be negative for $f = 1$. According to (40b), as Π is increased, $[G]_1^2$ first vanishes for $f = 1$ when

$$\Pi = \tfrac{1}{2}\kappa^2. \qquad (41)$$

Second, $[G]_1^2$ has a maximum value as a function of f; because positive values of $[G]_1^2$ correspond to an energy barrier to transformation, we see the connexion between the presence of this barrier, and the minimum occurring in the central pressure p_1.

To locate the maximum, we note that according to (40a), $[G]_1^2$ increases with f until $f = \kappa$ but subsequently decreases, as shown by (40b). So $[G]_1^2$ attains its maximum as a function of f at $f = \kappa$. As we have seen, for this value of κ, the stress at the outer edge of the rim is just small enough for deformation at the outer edge of the rim to be elastic.

The magnitude of this maximum is significant; if it is negative, transformation continues without stopping until the sample is completely converted. Substituting $f = \kappa$ into (40), we find that

$$\max_{0<f<1} [G]_1^2 = \tfrac{4}{3}\mu V \theta_T^2 \big(\tfrac{1}{2}\kappa^2 - \kappa \ln \kappa - \Pi\big). \tag{42}$$

This value is negative if the pressure ratio

$$\Pi > \tfrac{1}{2}\kappa^2 - \kappa \ln \kappa. \tag{43}$$

Because $\kappa \leq 1$, the pressure ratio (43) needed for the sample to convert completely is, of course, larger than the value (41) necessary for any product to form. Moreover, for a given value of Π, (43) can be satisfied by reducing κ, for example, by hydrating the sample; for fixed κ (fixed yield stress), it is satisfied if Π is sufficiently large. These two properties are used to interpret the next figure.

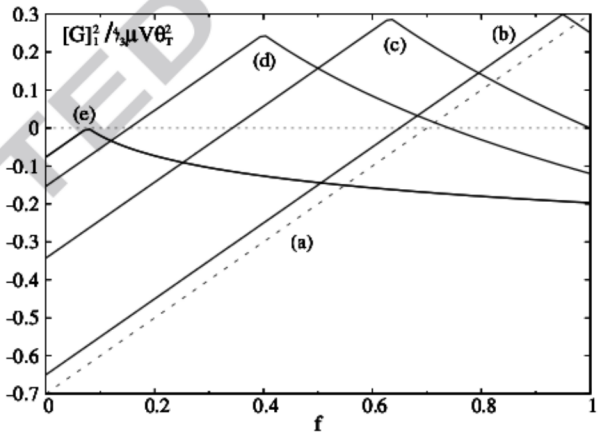

Figure 11: Potential difference calculated using (40) for $\Pi = 0.2$ and the following values of κ: (a) 1 (elastic), (b) 0.95, (c) 0.6325, (d) 0.4 and (e) 0.077. As defined by (25) and (37) respectively, $\Pi = -(p_a - \bar{p})/\frac{4}{3}\mu\theta_T$ and $\kappa = 3k/(4\mu|\theta_T|)$. For $[G]_1^2 < 0$, the phase interface propagates inwards consuming the parent phase. See text for discussion.

Figure 11 shows the potential difference $[G]_1^2$ as a function of volume fraction $f = R^3/b^3$ for $\Pi = 0.2$, and several values of κ. (For the values $\mu = 110$ GPa and $|\theta_T| = 0.06$ appropriate to wadsleyite at 1500 K and 15 GPa, this value of Π corresponds to an excess pressure of about 1.8 GPa.)

Cases (a) to (d) correspond to reducing the yield stress with fixed μ and θ_T. For case (a), shown as a broken line, deformation is purely elastic; transformation is impossible, at least in this geometry, because the value of Π lies within the forbidden range given by (27). For case (b), transformation still does not occur. Though part of the rim deforms plastically (because $\kappa < 1$), the potential difference is still positive for $f = 1$ because κ exceeds the critical value of $\sqrt{2\Pi}$ given by (43). Transformation first becomes possible for the critical case (c): now $[G]_1^2 = 0$ for $f = 1$.

Case (d) illustrates the situation in which transformation is able to begin, but subsequently stops. The sample transforms until the core pressure falls sufficiently to make $[G]_1^2$ increase to zero. According to (40b), $[G]_1^2 = 0$ for

$$f = \exp\left(\tfrac{1}{2}\kappa - \Pi/\kappa\right). \tag{44}$$

For the values $\Pi = 0.2$ and $\kappa = 0.4$ appropriate to curve (d), this value $f = 0.74$, as can also be seen from figure 11.

When transformation has stopped, as in case (d), the pressure within the central sphere still exceeds the Clapeyron pressure. Expressing (39b) in the form $\frac{p_1 - \bar{p}}{k} = \ln f + \Pi/\kappa$, then substituting for f from (44), we find that

$$\frac{p_1 - \bar{p}}{\frac{4}{3}\mu|\theta_T|} = \tfrac{1}{2}\kappa^2. \tag{45}$$

Comparing this with (41), we see that when rim growth ceases, the pressure within the central sphere is equal to that which must be applied to the outer sample surface in order for spherically–symmetric growth to be possible. Product grains could, therefore, grow within the inclusion if there are nucleation sites there. Unlike grains growing on the surface of single crystal, or on grain boundaries within a polycrystal, these isolated grains can adopt aspect ratios minimizing the strain energy. Although these isolated product grains suffer a nucleation penalty, they may perhaps permit unimpeded subsequent growth.

Lastly, curve (e) shows the potential difference for the marginal case in which $\max_f [G]_1^2 = 0$; by (43) the corresponding value of $\Pi = -\kappa \ln \kappa + \frac{1}{2}\kappa^2$.

The existence of case (e) has not previously been recognized. This case has an interesting feature: if Π is increased slightly, so as to satisfy (43), the sample will convert completely. Because the values of $[G]_1^2$ at $f = 1$ and at $f = 0$ are comparable, the initial and final interface speeds are comparable; however, because $[G]_1^2$ nearly vanishes, the sample will spend a long time near the maximum in $[G]_1^2$. The next figure illustrates this behaviour.

Figure 12 shows the radius R of the phase interface (expressed in units of sample radius b) as a function of time expressed in units $3b/(4\mu\lambda V\theta_T^2)$. These curves are obtained by solving numerically the kinetic equation (15) with the

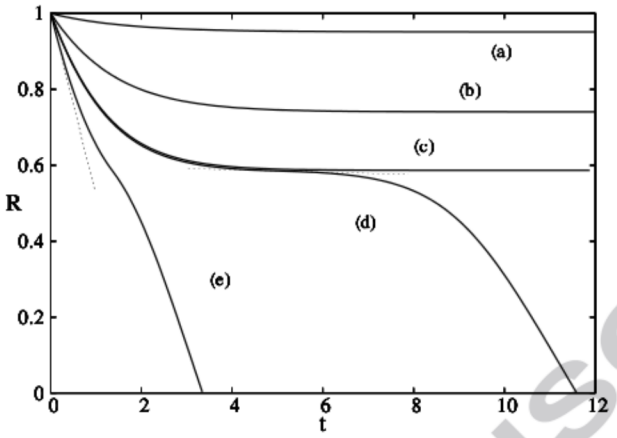

Figure 12: R as a function of dimensionless time t for $\kappa = 0.2$ and the following values of Π: (a) 0.05, (b) 0.2, (c) 0.34, (d) 0.345 and (e) 0.5. Broken lines, tangent to curve (e) at $t = 0$ and tangent to curve (d) at the point of minimum interface speed. As discussed in the text, the sample never converts in cases (a) to (c).

potential difference $[G]_1^2$ given by equation (40). The figure is drawn for $\kappa = 0.2$; for the values $\mu = 110$ GPa and $|\theta_T| = 0.06$ appropriate to the α–β transformation in olivine (1500 K, 15 GPa), $\kappa = 0.2$ corresponds to a stress difference $|\sigma_{rr} - \sigma_{\theta\theta}| = 2.6$ GPa. Curves (a) to (e) correspond to increasing the excess pressure $p_a - \bar{p}$ with all other parameters fixed; according to (43), for $\kappa = 0.2$, the sample can only convert completely if $\Pi > 0.3419$. For cases (a) to (c) $\Pi < 0.3419$, we see that for large t, R approaches the constant value determined by equation (44).

The behaviour in case (d) is quite different. Because the value of $\Pi = 0.345$ exceeds the critical value, the sample now converts completely. But, because Π exceeds the critical value only slightly, the maximum value of the potential difference is only slightly less than zero. As a result, the interface velocity decreases from its initial value to become nearly zero before increasing to a value comparable with its initial value. We note the following details of the behaviour near the point of least velocity.

According to our discussion of figure 11, the minimum value of $\mathrm{d}R/\mathrm{d}t$ occurs at $f = \kappa$; for $\kappa = 0.2$, this corresponds to $R = 0.5848$ and, from the numerical solution of the kinetic equation, we find R attains this value at time $t = 5.1081$. Using equation (42), we find that for $\kappa = 0.2$ and $\Pi = 0.345$, the corresponding value of the interface velocity is given by $\mathrm{d}R/\mathrm{d}t = \frac{1}{2}\kappa^2 - \kappa \ln \kappa - \Pi, = -0.003112$. In figure 12, the tangent to curve (d) through the point $t = 5.1081$ and $R = 0.5848$ is shown by the short broken line.

Lastly, curve (e) is included to show that if Π is sufficiently large (κ fixed), the sample converts at a nearly uniform velocity.

5. Transformation driven by slowly increasing Π

According to figure 12, if the pressure ratio Π is less than the critical value given by (43), the rim of product grows until R reaches the equilibrium value given by equation (44). In this steady state, the two phases are in equilibrium across their interface. Because equilibrium is attained on the timescale $t_s = 3b/(4\mu\lambda V\theta_T^2)$, if Π is now increased slowly, specifically, on a time scale large compared with t_s, the sample will pass through a series of equilibrium states in which the volume fraction f is given as a function of Π by equation (44). This process can continue until Π reaches the critical value. When Π exceeds that critical value, transformation can be completed rapidly on the time scale t_s; for example, although in case (d) of figure 12, Π exceeds the critical value by only 0.003112, the transformation is completed after a time $\sim 10t_s$. Increasing Π would, of course, result in even faster completion. Coupling of strain energy and kinetics therefore results in a separation of time scales when Π is increased slowly. Transformation is first delayed for the large amount of time needed for Π to attain the critical value. But, once that value is attained, transformation is rapid. This is the first quantitative example in which a long period of slow growth enabled by creep is followed by rapid complete transformation by elastic deformation.

6. Yield strengths inferred from experiment

Figure 13 shows published measurements of rim thickness x as a function of time. In all cases, the interface velocity decreases with time and, in some cases, the decrease is sufficiently strong that transformation appears to cease on the laboratory timescale. According to the kinetic relation (15), time–dependence of the interface velocity requires that the potential difference $[G]_1^2$ must itself vary with time.

Two explanations are possible for this variation. First, as expressed by equation (34a), deviatoric stresses within the sample could be large enough to generate pressure differences within the sample. Because an editor of this special volume has stated in a review of this paper that 'no pressure gradient should exist within a sample grain', we must examine the second possibility: the pressure p_a applied at the sample outer surface might itself have fallen over time. Though a constant hydraulic pressure is applied to the multianvil, as the sample transforms, the apparatus might be unable to adjust to the volume change. According to Rubie (1999, p.436), this may have occurred in experiments by Kerschhofer et al.(1998) in which a large single crystal of olivine was transformed using fine–grained olivine as the pressure medium. Because both the pressure medium and the sample underwent phase transformation, it is possible that the pressure on the sample surface actually fell as the pressure medium transformed. The hydraulic pressure was large enough that ringwoodite formed initially as the product phase but, after further transformation, the intermediate–pressure phase wadsleyite formed in the sample. That is consistent with a drop in the pressure on the sample surface.

For the experiments discussed here, however, the pressure medium is either halite (NaCl) or gold. Neither undergoes transformation at the experimental conditions (Boehler et al. 1997, figure 1; Young 1991, §13.10.3). In fact, the very behaviour found in these experiments is not consistent with a significant drop in p_a. Both Kubo et al.(1998b) and Diedrich et al.(2009) show experimentally that if a single crystal sample is sufficiently hydrated, transformation is rapid, and the interface velocity is independent of time; see, in particular, Diedrich et al. (2009, figure 9; also ¶3 on p.94). If the loading device could not maintain a constant pressure, that effect should have been most noticeable when the transformation is fastest. We conclude that the variation in potential difference must originate from pressure differences within the transforming sample itself. This leads us to interpret the data in terms of the present theory.

To this end, the function $x = c_0 - c_1 \exp(-c_2 t)$ was fitted to the data in figure 13. Values of the fitting constants c_0, c_1 and c_2 are given in the figure caption. The function $x(t)$ has a single timescale c_2^{-1}. To see the connection between that function and the theory, we note that in figures 13a, 13c and 13d (but not in 13b), transformation ceases on the laboratory timescale before the sample is completely transformed; the final rim thickness is also small compared with the sample radius. The appropriate function for $[G]_1^2$ is given by equation (40b) and, in that expression, we may linearize the kinetic equation by approximating $\ln f$ by $-3x/b$. (The maximum error in this approximation is about 16%; it occurs for the upper curve in figure 13a.) Thus simplified, the kinetic equation consisting of (15) and (40a) becomes

$$\frac{\mathrm{d}x}{\mathrm{d}t} = \lambda V|\theta_T|\Big\{\Delta p - \tfrac{3}{8}\frac{k^2}{\mu|\theta_T|} - 3\frac{k}{b}x\Big\}. \tag{46}$$

The fitting function satisfies this equation if we choose

$$c_2 = 3k\lambda|\theta_T|V/b \tag{47a}$$

and

$$c_0 = \tfrac{1}{3}b\Big\{\frac{\Delta p}{k} - \tfrac{3}{8}\frac{k}{\mu|\theta_T|}\Big\}. \tag{47b}$$

The remaining constant c_1 is determined by the initial rim thickness.

According to the theory, for the thin rims in figures 13a, 13c and 13d, rim thickness x grows on the timescale c_2^{-1}. This timescale is determined by the sample radius b, stress parameter k, kinetic constant λ, mean specific volume V of the parent and the product phase, and the fractional difference $|\theta_T|$ in specific volumes. For $c_2 t \gg 1$, the interface velocity vanishes exponentially with time, and the rim thickness approaches a final value of c_0. du Frane et al.(2013, figure 4b) show experimentally that, for their anhydrous samples, the interface velocity indeed vanishes exponentially with time.

The theory predicts that for a thin rim, growth occurs on a single timescale. Figure 13b is included as an example where that assumption is questionable. Though in this case, the rim is not thin, we may still use the function $x(t)$ as 3–parameter fitting curve. If, however, we extrapolate along the fitted curve,

we find that $x = 0$ at $t = -0.9$ hr. Either the authors missed the onset of rim growth by about an hour, or growth occurs initially on a timescale much shorter than the time scale of the order of a day or two on which transformation appears to completed in this case. It is clear that the elastic perfectly–plastic model does not describe this case well. This is consistent with the discussion in §1: for this series of experiments, Kubo et al.(1998b) observed the presence of well–defined subgrain boundaries, and inferred that the creep rate was enhanced.

By contrast, for the runs shown in the other figures 13a, 13c and 13d, the interface velocity decreases so rapidly with time that transformation ceases on the timescale of a few hours. Because the data appear to be consistent with the assumption of a single timescale, we use the theory to obtain the yield strength. Rearranging (47b), we obtain a quadratic equation determining k in terms of the fitting constant c_0, and the known quantities b, θ_T, μ and the excess pressure Δp. For this work, values of excess pressure Δp were obtained from values of values of the molar Gibbs energy difference ΔG_m and θ_T tabulated by Mosenfelder et al. (2001, table 1 and p.168): the relevant equation is $|\Delta G_m| = V_m \Delta p\, |\theta_T|$. For other properties, the following values were used: mean molar volume $V_m = 40$ cm^3/mol, rigidity $\mu = 110$ GPa (wadsleyite) and $\mu = 126$ GPa (ringwoodite).

rim	T K	p_a GPa	water ppmw	$p_a - \bar{p}$ GPa	f_∞	strain–rate$\times 10^5$ sec^{-1}	$\Delta\sigma$ GPa
Wd	1303[a]	13.5	200	0.43	0.71	0.6	1.6
	1503[a]	14.0		0.62	0.41	2	0.99
Rw	1273[b]	18.0	< 6	4.7	0.86		14
	1373[c]	18.0	'nom. anhydrous'	4.3	0.71		11

Table 1: Stress difference $\Delta\sigma = \sigma_{rr} - \sigma_{\theta\theta}$ calculated by applying equation (46) to the following experiments: *a*, Kubo et al.(1998a); *b*, du Frane et al.(2013); *c* Diedrich et al.(2009). Phases: wadsleyite (Wd) and ringwoodite (Rw).

As table 1, we give the stress difference $|\sigma_{rr} - \sigma_{\theta\theta}| = \frac{3}{2}k$ for the four cases included in figures 13a, 13c and 13d. The equilibrium volume fraction f_∞ given in the table is obtained from the value of c_0 given in the figure caption and the sample radius b using the equation $f_\infty = (1 - c_0/b)^3$. For the experiments of Kubo et al.(1998a), the table also includes an estimate of the initial strain–rate: evaluating the unnumbered equation below (28) at the phase interface, we find that the radial deviatoric strain is given in terms of interface velocity $\dot{R}$ and initial interface radius $R = b$ by $\dot{\gamma} = 2\theta_T \dot{R}/b$. Using the appropriate value of $\dot{R}$ obtained from the fitting curves, we find that the strain rate is about 10^{-5} sec^{-1}.

To demonstrate the validity of the analysis, we first discuss the results for wadsleyite, and compare them with independent measurements. We then discuss the implausibly large values obtained for ringwoodite.

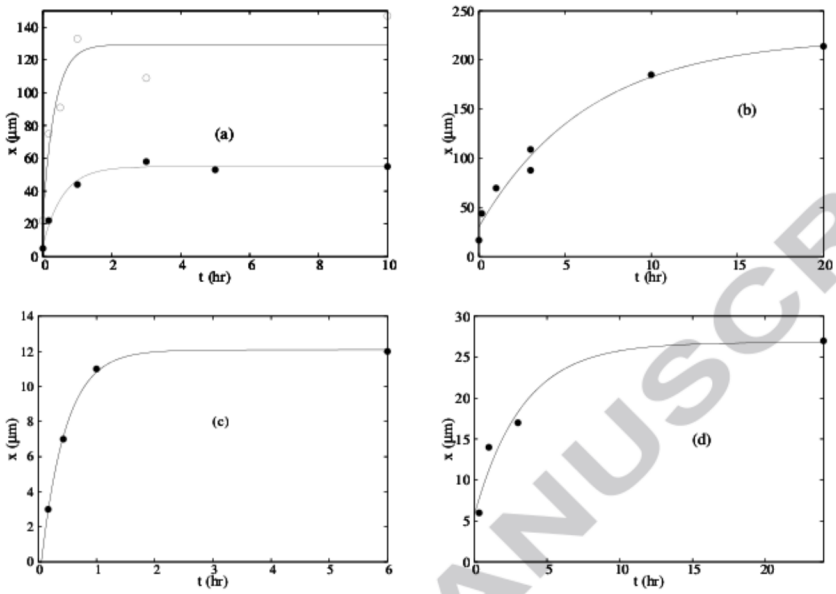

Figure 13: Rim thickness as a function of time: curves are fitted. Figures (a) and (b): wadsleyite rim grown on a 1 mm olivine cube. (a) Kubo et al.(1998a, table 1) 200 ppmw. • 1303 K, 13.5 GPa: $c_0 = 55.0$ μm, $c_1 = 48.1$ μm, $c_2 = 1.73$ hr$^{\pm 1}$; ∘ 1503 K, 14 GPa: $c_0 = 129$, $c_1 = 104$, $c_2 = 2.84$. (b) Kubo et al.(1998b figure 2) 500 ppmw. 1303 K, 13.5 GPa: $c_0 = 223.0$, $c_1 = 193$, $c_2 = 0.157$. Figures (c) and (d): ringwoodite rim grown on a 0.5 mm olivine sphere. (c) du Frane et al.(2013, table 2, 'method 2') < 6 ppmw. 1273 K, 18 GPa: $c_0 = 12.1$, $c_1 = 13.7$, $c_2 = 2.37$. (d) Diedrich et al.(2009, table 1) 'anhydrous'. 1373 K, 18 GPa: $c_0 = 26.8$, $c_1 = 21.1$, $c_2 = 0.302$

6.1. Yield strength of wadsleyite

As their figure 7, Kawazoe et al.(2010) show wadsleyite yield strength measured as a function of strain using a rotational Drickamer apparatus. At a strain rate comparable with that given in table 1, the stress in their sample B040 (23 ppmw H_2O) at 15.1 GPa and 1690 K is about 2.2 GPa after 4% strain. This is about twice the value given in table 1 for the Kubo et al. series at 14.0 GPa and 1503 K. We note that, unlike the Kubo et al. sample, that of Kawazoe et al. is essentially anhydrous; the other experimental conditions are fairly close.

The factor of two difference in yield strength is qualitatively consistent with the experiments of Chen et al.(1998a,b) on synthetic wadsleyite: at 873 K and 10 GPa, the stress in their anhydrous sample is about 1.5 times that in their sample containing 3.8 ppmw of water. (It is unfortunate that, apparently based on their abstract, the Chen et al. experiments have been described as showing that water has only a slight effect on yield strength. This is only true of their low temperature experiments, however: 'the hydrous phase remains as strong

as the anhydrous phase at temperatures up to 400° C. . . upon further heating to 600°C,the hydrous phase begins to weaken relative to the anhydrous phase.' (Chen et al. 1998, p.1104). Overall, these three studies appear compatible.

The dislocations observed in the wadsleyite rim are of, of course, likely to have a different origin than those occurring in deformation experiments not involving phase change. As noted below equation (6) of this paper, in the product rim, the maximum *radial* deviatoric strain occurs at the phase interface: that maximum is of the order of 4% for the olivine–wadselyite transformation. Though, in their deformation experiments, Kawazoe et al.(2010, figure 7) observed that stress reached steady state after a strain of about 5%, the strain history is quite different in the two processes. In their case, strain increases with time. During rim growth, by contrast, the radial deviatoric strain of a wadsleyite particle is greatest in magnitude at the phase interface; it then decreases as the interface propagates further into the sample. With that caveat, however, we note that similar dislocation structures are, in fact, observed in the two processes.

Kawazoe et al.(2010, ¶26) describe in their recovered samples as follows: 'the microstructures in the lower temperature samples are characterized by the formation of dislocation cell structures that are composed of heavily tangled dislocation cell walls. . . this microstructure suggests that deformation at the lower temperatures involves only dislocation glide without much effect of recovery'. As discussed already in §1, Kubo et al. use similar words to describe the structures observed in the rim of wadsleyite product: see also Kubo et al. (1998b, figure 5). (To avoid confusion, we note that in the Kawazoe et al. study, the lowest temperature was 1670 K.) Similarly, Thurel et al. (2003) deformed wadsleyite at 1573 K and 14 GPa to plastic strains of between 60% and 73%; like Kawazoe et al., they deduced that dislocation glide was the dominant mechanism allowing plastic strain. Available evidence is consistent with the dislocation structures, and the yield strength both being similar in the two processes.

We must note a contrary view. Mosenfelder et al.(2000) conclude that in their wadsleyite rims grown at 1373 K and 17 GPa, 'the presence of organized cell walls suggests that dislocation climb is rapid, even at the relatively low temperature of the experiments'. They do not comment on the difference between the microstructure they observed, and the tangled dislocations observed by Kubo et al. at an only slightly lower temperature of 1303 K. Though Kubo et al.(1998b) observed the presence of organized cell walls in their wet experiments (500 ppmw of water), Mosenfelder et al.(2000, p.65) state that the hydrogen content of their starting material (san Carlos olivine) was less than 10 $H/10^6$ Si. Because that is about one–fortieth the hydrogen content of the (annealed) Kawazoe et al. sample discussed above, it appears that the Mosenfelder et al. observations are not due to water content.

Assuming ideal plasticity, Mosenfelder et al.(2000, p.70) model the Kubo et al. experiments. They infer a 'yield strength between 3 and 5 GPa for nominally dry experiments at 1030° C to 1330° C'. Their estimates are about 3 times those given in table 1. Thurel et al.(2003) describe the Mosenfelder et al. values as being 'surprisingly high' and suggest the different origins of the

dislocation structures as an explanation. That is not a convincing explanation. The Mosenfelder et al. estimates are based almost entirely on the experiments of Kubo et al.; as discussed above, Kubo et al. observed dislocation structures closely resembling those in the experiments of Kawazoe et al. (2010). In the appendix, it is shown that Mosenfelder et al. analysis is not consistent with our discussion of kinematics in §2. Given that error in their analysis, it is not worth speculating further as to the cause of their 'surprisingly high' estimate for wadsleyite strength.

6.2. Yield strength for ringwoodite

According to figure 13, ringwoodite rims grow to a thickness of 10–20 μm, and growth then appears to stop. Because the rim thickness is small compared with the sample radius, equation (46) still applies. But from table 1, we see that the yield strengths required to explain the observed rim thicknesses are implausibly large: they are comparable with the ideal strength (Karato 2008, §5.1). For comparison, Chen et al. (1998a) report a yield strength of the order of $\mu/100$ for fine–grained ($\sim 1\,\mu$m) polycrystalline anhydrous ringwoodite at 1273 K and 20 GPa. Because this value is comparable with that for wadsleyite, whereas the excess pressure is about 10 times that for the wadsleyite experiments, we would to see expect thicker rims for ringwoodite. In fact, the discrepancy is even worse than that. For the parameter values given above table 1, and an assumed value $k = 1$ GPa, corresponding to a stress difference of 1.5 GPa similar to that observed by Chen et al., we find by solving the kinetic equation (without the thin rim approximation) that the rim grows without stopping until the sample is completely transformed. I have no explanation for the discrepancy.

Though we have taken the phases to be incompressible, it is not obvious why this assumption should become fatal for modelling ringwoodite while still giving credible values for wadsleyite.

7. Summary

7.1. Kinematics

Because the rheology of the product rim is poorly known, here we have reduced the problem of determining the strain field to its simplest nontrivial form. In the case of incompressible phases, and spherically–symmetric deformation, the deformation is determined by conservation of mass. This simplification allows us to determine the strain before introducing assumptions about rheology. Our results therefore provide a critical test of studies in which rheological assumptions are included in the initial formulation of the model (Liu et al.1998, Mosenfelder et al. 2000, Morris 2002). In the appendix, it is shown that, owing to errors in formulation, each of those studies leads to incorrect conclusions.

In particular, we have shown here that the radial deviatoric strain e'_{rr} within the rim of dense product is negative (compressive) and, further, that the value taken by e'_{rr} at the phase interface is independent of time: according to equation

(8), no matter how far the phase interface has propagated, at the interface e'_{rr} is equal to two–thirds the fractional difference in the specific volume of the phases.

We have also shown that within the product rim, the *rate* of radial deviatoric strain is positive (tensile), i.e. it is of opposite sign to the strain. Using equation (6b), we have explained that the strain experienced by an element of material can be negative even though the rate of strain within the rim is positive: during its transformation, the element of material suffers an impulsive compressive deviatoric strain, and the subsequent positive rate of strain experienced by the element serves to reduce the magnitude of the deviatoric strain to its ultimate value of zero.

Once we introduce rheology, the difference in sign between deviatoric strain, and rate of deviatoric strain is important.

7.2. Metastability of elastic phases

Owing to the large deviatoric strain suffered by an element as it is transformed, the material is unlikely to behave elastically. It is, however, essential to understand the behaviour of the elastic system as a standard against which to interpret the effects of creep.

According to accepted results, the propagation speed of the phase interface is proportional to the increment $[G]_1^2 = G_2 - G_1$ in thermodynamic potential of a unit mass of material when it transforms from parent phase 1 to product phase 2. For our model geometry, $[G]_1^2$ is related to the Helmholtz free energy F, specific volume V, and to the hydrostatic pressure p_1 within the core phase by equation (17):

$$[G]_1^2 = [F - \bar{F}]_1^2 + (p_1 - \bar{p})[V]_1^2; \qquad (17')$$

$\bar{p}$ denotes the pressure at which the phases coexist in a common hydrostatic state, and $\bar{F}$ denotes the Helmholtz free energy for that state. According to (17), when an element of material is transformed, the increment in G is equal to the sum of the increment in Helmholtz free energy, and the pressure–volume work performed on the element during its compression.

Elastic strain within the rim of dense product affects these contributions in opposite senses. Because the radial deviatoric strain is compressive there, the core pressure p_1 exceeds the applied pressure p_a when the phases are elastic. As a result, when unit mass of less–dense phase 1 is converted to the denser phase 2, the work done is negative; in an elastic material, the pressure–volume term $(p_1 - \bar{p})[V]_1^2$ represents an effect tending to drive transformation.

By contrast, deviatoric stress within the rim acts to increase the Helmholtz free energy F of the product (rim) phase relative to that of the parent (core) phase. Because converting unit mass of less–dense phase to the denser phase stores potential energy within the strained phase, the Helmholtz free energy represents an effect tending to impede transformation (at least in our geometry).

According to equation (27), as a result of these competing effects, there is a range of excess pressures within which the elastic model exhibits hysteresis; low–pressure phase can exist metastably at pressures exceeding the Clapeyron pressure $\bar{p}$ at which the phases coexist in a common hydrostatic state. Applied

to the α–β transformation in olivine, equation (27) predicts that if the phases behave elastically, either phase could exist metastably over over a pressure range of almost 9 GPa. (Compressibility of the phases will reduce the magnitude of this pressure range.)

Qualitatively different behaviour is predicted by the Liu et al.(1998) analysis: according to it, within the rim, strain develops from an initial value of zero. As a result, some transformation occurs before the interface stops propagating; see their figure 5. Although that result is qualitatively consistent with the Kubo et al.(1998a) experiments, because the Liu et al. conclusions about the strain are erroneous, we still need an explanation of those experiments.

According to Kubo et al., plastic flow occurred even in the experiment at 1303 K and 13.5 GPa for which growth stopped on the laboratory. This suggests that rather than becoming significant following a period of elastic strain in the manner suggested by Rubie and Thompson, plastic flow might be essential throughout the entire transformation. We have therefore analysed growth in a perfectly plastic solid, the object being to understand the overall behaviour to be expected, rather than to model the experiments in detail. To this end, we have assumed the phases to be incompressible, so that the displacement is still given by the results in §2.

7.3. Perfect plasticity

We have shown that plastic flow has two opposing effects. It tends to facilitate transformation by reducing the elastic component of strain within the product; by reducing the potential energy stored per unit mass of product, creep reduces the energetic cost of transformation. It tends to impede transformation by countering the increase in core pressure that, as we have seen, would occur if the material were elastic. The potential curves shown in figure 11 express the competition between these opposing effects.

The first of these effects is essential to allowing transformation to begin. For a product rim of negligibly small thickness (volume fraction of parent phase $f \to 1$), the pressure difference across the rim is vanishingly small (equation 39b), and the only possible effect of yielding is to reduce the potential energy increase resulting from transformation. Indeed, as we see from equation (41b), at $f = 1$, yielding ($\kappa < 1$) reduces the energy barrier and tends to facilitate the onset of transformation. For a given value of yield stress, a product rim (of vanishing thickness) forms if the excess pressure exceeds the critical value given by equation (41).

Once the product rim exists, the reduction in core pressure comes into play. As transformation proceeds, the volume fraction of parent phase is reduced, and the rim thickens. As a result, the core pressure drops and the energy barrier increases. According to figure 11, $[G]_1^2$ does not increase monotonically as f is reduced; instead $[G]_1^2$ has a maximum value. Thie maximum exists because when the rim becomes sufficiently thick, the deviatoric stress in its outer part falls below the yield stress. Across the outer elastic shell, the pressure difference is opposite in sign to that occurring across the plastic region, owing to the sign of the deviatoric radial stress (equation 39). As a result, when the rim is

sufficiently thick, the core pressure *rises* rather than falling as transformation proceeds. This tends to promote transformation; the effect is manifested as a maximum in $[G]_1^2$.

There are now two possibilities: if the maximum height of the energy barrier is positive, transformation stops, leaving a product rim in *apparent* thermodynamic equilibrium with a core of parent; if the maximum is negative, transformation will continue to completion, although the propagation speed will decrease as the sample passes over what is left of the energy barrier. This behaviour is shown in figure 12.

7.4. Implications for modelling deep earthquakes

As discussed at the end of §1, in laboratory experiments on rim growth, the deviatoric stress is sufficiently large to cause the material to deform plastically even though the homologous temperature is of the order of 0.5 or greater. When a material deforms by low–temperature plasticity, strain–rate depends strongly on the deviatoric stress. Because, in an experiment designed to allow a phenomenon to be observed within a given time interval, the strain–rate is fixed in order of magnitude, it follows that for processes governed by low–temperature plasticty, and occurring on a single timescale, the deviatoric stress is essentially fixed in magnitude. This provides the motivation for the theory of ideal plasticity.

Using this theory, we have shown (figure 12) that, depending on the magnitudes of the dimensionless excess pressure and dimensionless yield strength, several behaviours are possible. For the purpose of illustration, in that figure, let us choose the range $0 < t < 4$ to be the window within which experiments can be performed. There is now a single timescale, set by our choice of window. Within that window, the theory of ideal plasticity makes sense. However, our model also makes two predictions concerning the behaviour outside that window. Although the predictions lie outside the range of validity of the simplified theory, they are suggestive, and they serve to motivate the effort of developing a more realistic theory.

According to figure 12, we see that for a certain range of yield strengths, transformation is predicted to stop (on the timescale set by our window). Evidently, in that case, the system will relax to allow growth on a longer timescale. (In Morris 2002, I attempted to model that process of growth on two timescales: though, as we discuss in the appendix to this work, my earlier analysis contains errors, the underlying physical problem remains important.) Based on the analysis given by Morris (1995, p.347), we expect the yield strength to decrease as the strain falls, and so to allow transformation on a longer timescale. In that case, we expect a slow relaxation of the system as the transformation is completed.

The second type of behaviour predicted in figure 12 may be connected with the occurrence of deep earthquakes. According to this simplified model of ideal plasticity, there is a range of excess pressures within the sample first transforms on the timescale set by the time window; the growth rate then drops almost to zero over a period that can be long; but then growth begins again on the

timescale set by the window. To understand what happens in the middle period of slow, almost imperceptible growth, we need now to include a more complete description of low–temperature plasticity, along the lines given in Morris (1995). Because the underlying issues in this problem are now more clear, it will be appropriate to include the effects of compressibility of the phases in the next stage of this work.

In subduction zones, the pressure applied to a sample increases quasi–statically as the slab is subducted. That is the motivation for the discussion in §5. There I argue physically that if the excess pressure on a sample is increased quasistatically, the sample will pass through a series of thermodynamic equilibria with a product rim of gradually increasing thickness. According to the simplified model provided by ideal plasticity, this gentle process will continue until a certain critical pressure is reached. Rapid transformation then becomes possible on the timescale set by interface kinetics, rather than rheology.

All this is based on a simplified model provided by the theory of ideal plasticity. Though the issues needed to be analysed in that model are obvious, without that model, the questions would not even be formulated. We have not even touched on the relation between rim growth on single crystals, and rim growth in polycrystalline samples.

This work is dedicated to Professor Robert Liebermann. I am grateful to the editors for their comments which have helped (I hope) improve my presentation; and, above all, to Dr. Tomoaki Kubo for a signed review of this work and for his having responded to my questions over many years.

Appendix: causality and the formulation of the constitutive equation

In this appendix, results obtained from published papers are denoted by an asterisk.

In §1, we state that causality can be violated if the constitutive equation is incorrectly formulated. In this paper, causality is imposed on each of the constitutive models. For the elastic case, this is done above equation (10) when we take the deviatoric stress within a phase to be determined by the deviatoric strain occurring within that phase. For ideal plasticity, causality is imposed when we integrate the incremental form of Hooke's law (equation 29), because the integration is made between states of a given phase.

This approach is equivalent to that of Lee and Tromp (1995). To model the effect of density changes caused by metamictization (expansion caused by radiation damage to crystal structure), those authors consider a composite sphere comprising 3 concentric spherical shells each having arbitrary elastic constants. The radii of the shells are assumed to be independent of time, the density change occurring simultaneously throughout the entire shell of interest. Though that process differs from the one considered here, in which the density change occurs at a propagating interface of radius R, for a given value of R the state of the system is the same. By specializing the Lee and Tromp results to the case of two incompressible shells, the outer one of which has undergone a spatially uniform

density change from its initial state, we can legitimately compare the solutions. Evaluating their equations (A3) to (A7) for the case $K_1 = K_2$, $\mu_3/K_2 \to 0$ (fixed K_2/K_3), we find that their result giving displacement in the rim is equivalent to our (2b). Like our result, the Lee and Tromp result is consistent with the theory of infinitesimal strain. As for imposing causality, when Lee and Tromp formulate their constitutive equation (their equation 24), they take the stress tensor for a given shell to vanish if the strain in that shell is equal to the transformation strain. This is equivalent to the argument leading to our equation (10).

The formulation of Liu et al.(1998) provides an example of a formulation which violates causality, by contrast. They analyse growth of a rim of dense phase assuming linear elasticity; their results are given for arbitrary Poisson ratio ν. For the special case of incompressible phases ($\nu = 1/2$), their equations (3) and (7) predict the following displacement:

$$u^* = \begin{cases} \varepsilon^* r, & r < R; \\ \varepsilon^* \frac{R^3}{r^2}, & r > R. \end{cases} \qquad (A.1)$$

As defined by their (2), $\varepsilon^* = \theta_T(R_0^3 - R^3)/(3R^3)$, where R_0 is the value of R at $t = 0$.

The Liu et al. result is not consistent with the theory of infinitesimal strain, according to which the fractional change in volume of a particle from its initial to its current state is given by the divergence of the displacement field. From equation (A.1), we obtain

$$\operatorname{div} \mathbf{u}^* = \begin{cases} 3\varepsilon^*, & r < R; \\ 0, & r > R. \end{cases} \qquad (A.2)$$

We see that causality is violated: within the central sphere of parent phase div $\mathbf{u}^* \neq 0$, even though no particle of the incompressible phase there has yet changed its volume. Within the product rim, by contrast, div $\mathbf{u}^* = 0$, even though each particle of product has in fact changed volume during transformation.

That error originates in the argument used by Liu et al. to obtain their (4) from their (3). That argument closely follows that used by Lee et al. (1980) to obtain their equation (7). The physical situation is, however, essentially different: Lee et al. analyse growth of an isolated sphere of product, whereas Liu et al. are treating growth of a product rim. In the first case, all material within the central sphere a change in volume; in the second case, it has not. The Liu et al. formulation should have reflected that essential difference.

The Liu et al. calculation incorrectly predicts the sign of the radial deviatoric strain. According to (A.1), within the rim the radial deviatoric strain is given ${e'_{rr}}^* = -2\varepsilon^* R^3/r^3$; because $\varepsilon^* < 0$, the radial deviatoric strain is predicted to be positive (tensile). Further, at the phase interface ${e'_{rr}}^* = -2\varepsilon^*$; the radial deviatoric strain there develops from an initial value of zero and ultimately becomes infinite as $R \to 0$. Liu et al. (1998, p.23906) emphasize the importance of this behaviour for their interpretation of the experiments. By

contrast, according to the correct expression (6), the radial deviatoric strain at the interface is finite and independent of time.

Mosenfelder et al. (2000) also give results disagreeing with the theory of infinitesimal strain. For example, specializing their (A12) to the case of incompressible phases (infinite bulk modulus), we find that the displacement within the plastic region of the product rim is given by $u^* = c_3/r^2$, where c_3 is independent of r. Consequently div $\mathbf{u}^* = 0$; the divergence of their displacement field is zero even though each particle within the product rim has undergone a volume change from its initial state.

In Morris (2002, p.1373) it is concluded that, within the rim of dense product, 'radial strain rate is tensile, and a tensile radial stress develops in accordance with the flow rule'. Though the first clause in this statement is correct, the second part is *incorrect* whenever strain has a significant effect. Though the expression given for strain–rate (Morris 2002, p.1370) is correct, in using it, I did not recognize that the strain itself is discontinuous at the phase interface.

To show the significance of that discontinuity, we compare the strain–rate calculated from the correct expression (6) of the present work with that given in Morris (2002). Because the strain is infinitesimal, the strain–rate may be obtained by differentiating (6) with respect to t (fixed r). To represent the strain discontinuity, we introduce the Heaviside unit step: $H(r-R) = 1$ for $r > R$ but is zero otherwise.

Expressing (6a) and (6b) in the form

$$e'_{rr} = \tfrac{2}{3}\theta_T \frac{R^3}{r^3}\, H(r-R),$$

then taking the partial derivative with respect to t, we obtain

$$\frac{\partial e'_{rr}}{\partial t} = 2\theta_T \frac{\mathrm{d}R}{\mathrm{d}t}\Big\{\frac{R^2}{r^3}\, H(r-R) - \tfrac{1}{3}\delta(r-R)\Big\}. \qquad (A.3)$$

Here $\delta(r-R)$ denotes the Dirac delta function, and we have used the property $f(x)\,\delta(x) = f(0)\delta(x)$.

The first term on the right hand side of (A.3) represents the deviatoric strain rate within the rim for $r > R$. The expression given in Morris (2002, p.1370) is equivalent to this term; for an inward growing dense rim, it represents a positive (tensile) strain–rate. But although the strain–rate is tensile throughout the rim, the strain itself is compressive there.

The second term in (A.3) explains the difference. It describes the impulsive compressive radial deviatoric strain–rate experienced by an element as it is transformed. The subsequent tensile strain–rate experienced by the element within the rim following its transformation asymptotically reduces that radial deviatoric strain to zero. This is consistent with (6a). According to it, the deviatoric radial strain vanishes as $R \to 0$ at fixed position r. Because the expression given in Morris (2002) does not include the impulsive contribution, integrating it with respect to t does not give the total strain experienced by a particle. Further, though the first term in (A1) is separable (it is the product

of a function of t with a function of r), the missing term is not separable. As a result, conclusions drawn from the separable solution (Morris 2002, equation 3a) are, to the extent that they depend upon the strain field, incorrect.

References

[0] Boehler R., Ross M., and Boercker D.B. 1997. Melting of LiF and NaCl to 1 Mbar: systematics of ionic solids at extreme conditions. *Phys. Rev. Lett.* 78, 4589–4592.

[0] Chen J., Inoue T., Weidner D.J., Wu Y. and Vaughan M.T. 1998. Strength and water weakening of mantle minerals, olivine, wadsleyite and ringwoodite. Geophys. Res. Lett. 25, 575–578.

[0] Diedrich T, Sharp TG, Leinenweber K and Holloway JR. 2009. The effect of small amounts of H_2O on olivine to ringwoodite transformation growth rates and implications for subduction of metastable olivine. *Chem. Geology* 262, 87–99.

[0] du Frane, W.L., Sharp, T.G., Mosenfelder, J.L. and Leinenweber, K. 2013. Ringwoodite growth rates from olivine with 75 ppmw H_2O. *Physics Earth Planet. Inter.* 219, 1–10.

[0] Evans, B. and Goetze, C. 1979. The temperature variation of the hardness of olivine and its implication for polycrystalline yield stress. *J. Geophys. Res.* 84, 5505–5524.

[0] Gibbs J.W. 1928. *Collected Works*. Volume 1. Thermodynamics. Longmans, Green.

[0] Gillet P, Gérard Y and Willaime C. 1987. The calcite–aragonite transition: mechanisms and microstructures induced by the transformation stresses and strain. *Bull. Minéral.* 110, 481–496.

[0] Green, H.W. 1986. Phase transformation under stress and volume transfer creep. In *Mineral and Rock Deformation: Laboratory Studies*. Geophys. Monogr. Ser. Vol.36. Eds B.E. Hobbs and H. Heard, pp. 201–211. American Geophysical Union.

[0] Heidug, W. and Lehner, F.K. 1985. Thermodynamics of coherent phase transformations in nonhydrostatically stressed solids. *PAGEOPH* 123, 91–98.

[0] Karato, S.–I. 2008. *Deformation of Earth Materials*. Cambridge.

[0] Kawazoe T., Karato S.–i., Ando J.–i. and Jing Z. 2010. Shear deformation of polycrystalline wadsleyite up to 2100 K at 14–17 GPa using a rotational Drickamer apparatus. *J. Geophys. Res.* 115 B08208.

[0] Kubo T., Ohtani E., Kato T., Shinmei T., and Fujino K., 1998a. Experimental investigation of the α–β transformation of San Carlos olivine single crystal, *Phys. Chem. Miner.*, 26, 1-6.

[0] Kubo T., Ohtani E., Kato T., Shinmei T., Fujino K. 1998b. Effects of water on the transformation kinetics in San Carlos olivine. *Science* 281, 85–87.

[0] Lee J.K., Earmme Y.Y., Aaronson H.I. and Russell K.C. 1980. Plastic relaxation of the transformation strain energy of a misfitting spherical precipitate: ideal plastic behaviour. *Met. Trans.* 11A, 1839–1847.

[0] Lee J.K.W. and Tromp J. 1995. Self–induced fracture generation in zircon. *J. Geophys. Res.* 100, 17 753–17 770.

[0] Liu M., Kerschhofer L., Mosenfelder J.L. and Rubie D.C. 1998. The effect of strain energy on growth rates during the olivine–spinel transformation and implications for olivine metastability in subducting slabs. *J. Geophys. Res.* 103, 23 897–23 909.

[0] Love A.E.H. 1927. *A Treatise on the Mathematical Theory of Elasticity.* 4th ed. Cambridge. (Dover reprint 1944).

[0] Morris S. 1992. Stress relief during solid–state transformations in minerals. *Proc. R. Soc. Lond.* A 436, 203–216.

[0] Morris S. 1995. The relaxation of a decompressed inclusion. *Z. angew. Math. Phys.* 46, S335–S355.

[0] Morris S.J.S. 2002. Coupling of interface kinetics and transformation–induced strain during pressure–induced solid–solid phase changes. *J. Mech. Phys. Solids* 50, 1363–1395.

[0] Mosenfelder J.L. and Bohlen S.R. 1997. Kinetics of the coesite to quartz transformation. *Earth Planet. Sci. Lett.* 153, 133–147.

[0] Mosenfelder J.L., Connolly J.A.D., David C. Rubie D.C. and Liu M. 2000. Strength of $(Mg,Fe)_2SiO_4$ wadsleyite determined by relaxation of transformation stress. *Phys. Earth Planet. Inter.* 120, 63–78.

[0] Paterson M.S. 1973. Nonhydrostatic thermodynamics and its geologic applications. *Rev. Geophys. Space Phys.* 11, 355–389.

[0] Rubie, D.C. and Thompson A.B. 1985. Kinetics of metamorphic reactions at elevated temperatures and pressures: an appraisal of available experimental data. In 'Metamorphic Reactions: Kinetics, Textures and Deformation' ed. A.B. Thompson & D.C. Rubie. Springer.

[0] Rubie, D.C. and Champness, P. E. 1987. The evolution of microstructure during the transformation of Mg_2GeO_4 olivine to spinel. *Bull. Minéral* 110, 471-480.

[0] Rubie, D.C. 1999. Characterizing the sample environment in multianvil high–pressure experiments. *Phase Transitions*, 68, 431–451.

[0] Schmid D.W., Abart R., Podladchikov Y. and Milke, T. 2009. Matrix rheology effects on reaction rim growth II: coupled diffusion and creep model. *J. metamorphic Geol.* 27, 83–91.

[0] Thurel E., P. Cordier P., Frost D. and Karato S.–I. 2003. Plastic deformation of wadsleyite: II. High–pressure deformation in shear. *Phys. Chem. Minerals* 30, 267–270.

[0] Truskinovskiy L.M. 1984. The equilibrium between a spherical nucleus and the matrix in a solid–state transformation. *Geochem. Int.* 21, 14–18.

[0] Vaughan P.J., Green H.W. and Coe R.S. 1984. Anisotropic growth in the olivine–spinel transformation of Mg_2GeO_4 under nonhydrostatic stress. *Tectonophysics* 108, 299–322.

[0] Young D.A. 1991. *Phase Diagrams of the Elements*. University of California Press.